Politecnico di Milano

SCHOOL OF INDUSTRIAL AND INFORMATION ENGINEERING

Master of Science – Biomedical Engineering

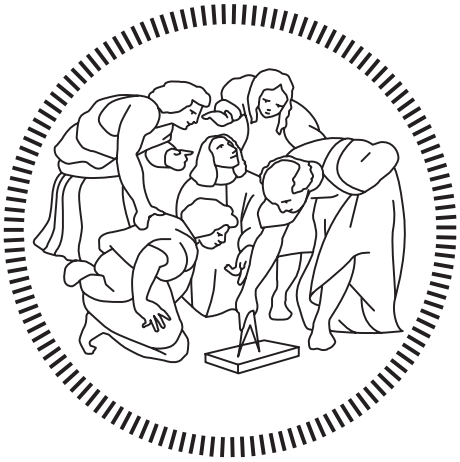

Design of an orthosis for the application of a myoelectrically driven FES device for tetraplegic users

Supervisor

Prof. Carlo FRIGO

Co-Supervisor

Ing. Rune THORSEN

Candidate

Sara SCOLARI – 10459374

Academic Year 2019 – 2020

ABSTRACT

This thesis project was carried out at the Don Carlo Gnocchi Foundation and concerns the development of an orthosis for the forearm that supports the MeCFES device, a functional electrical stimulator with myoelectric control, to facilitate its application in tetraplegic subjects. Tetraplegia occurs in the case of spinal injuries at the cervical level, manifests itself with total or partial paralysis of the limbs and involves a drastic reduction in the quality of life. People with this pathology have great difficulty in carrying out many daily actions independently. Thanks to MeCFES, it is possible to restore the grip capacity of the hand, and therefore restore the autonomy of the users to whom it is addressed.

The developed orthosis aims to position the electrodes for stimulation and the detection of the myoelectric signal in the correct points of the forearm automatically so that users can wear this technology by themselves.

The design has directly involved consumers in order to meet their specific needs to overcome the problem of common disuse in assistive devices in the rehabilitation field. To overcome the economic barrier imposed by products that integrate similar technologies on the market, it was decided to make the device do-it-yourself: a design was therefore studied using the software Onshape, which allows free signup and editing of the shared document via cloud services, and instructions for its 3D printing and for the assembly of its components have been reported.

To validate the models, the following project requirements have been set:

- Optimal fit, to keep the electrodes firmly in position in contact with the arm, to optimize the conduction of stimulation and avoid motion artefacts.
- Support the physiological movements of the forearm, especially pronation and supination.
- Comfortable, to be worn daily.
- Easily worn independently by the user.
- Do-it-yourself.
- Low cost

The prototypes were realized thanks to the 3D printers made available by the research institute, and these were optimized in a joint way involving the Don Gnocchi team and a volunteer suffering from tetraplegia, met through the Niguarda hospital in Milan.
As regards the final model, simulations were carried out with the Abaqus / CAE software to validate the choice of material and, through three-dimensional reconstruction of the forearm of four collaborators, the fit of the model was evaluated. A prototype was printed for one of these candidates, and the assembly and fit tests were carried out.
It was therefore possible to verify that the prototype met the requirements.

SOMMARIO

Questo progetto di tesi è stato realizzato presso la Fondazione Don Carlo Gnocchi e riguarda lo sviluppo di un'ortesi per l'avambraccio che supporti il dispositivo MeCFES, uno stimolatore elettrico funzionale con controllo mioelettrico, per facilitarne l'applicazione in soggetti tetraplegici. La tetraplegia si verifica in caso di lesioni spinali a livello cervicale, si manifesta con la paralisi totale o parziale degli arti e comporta una drastica riduzione della qualità di vita. Le persone affette da questa patologia, infatti, hanno grandi difficoltà a svolgere in autonomia molte azioni quotidiane. Grazie al MeCFES può essere rinstaurata la capacità prensile della mano, e quindi restituire indipendenza agli utenti a cui esso è rivolto. L'ortesi sviluppata ha l'obbiettivo di posizionare gli elettrodi per la stimolazione e per la rilevazione del segnale mioelettrico nei punti dell'avambraccio corretti in maniera automatica, in modo che gli utenti possano indossare questa tecnologia autonomamente. La progettazione ha coinvolto direttamente i consumatori, in modo da andare incontro alle loro esigenze specifiche per superare la problematica del disuso comune nei dispositivi di assistenza in ambito riabilitativo. Per superare inoltre la barriera economica imposta dai prodotti che integrano simili tecnologie in commercio, si è pensato di rendere il dispositivo fai da te: è stato quindi studiato un design tramite il software Onshape, che consente la registrazione gratuita e la modifica del documento condiviso tramite servizi cloud, e sono state riportate le istruzioni per la sua stampa in 3D e per l'assemblaggio delle sue componenti. Per validare i modelli, sono stati sono stati considerati i seguenti requisiti di progetto:

- vestibilità ottimale, per tenere gli elettrodi saldamente in posizione sull'avambraccio e consentire la corretta stimolazione ed evitare artefatti da movimento

- supporto dei movimenti fisiologici dell'avambraccio, in particolare la pronazione e la supinazione.
- Confortevole, per uso quotidiano.
- facilmente indossabile autonomamente dall'utente.
- Fai da te
- Basso costo

I prototipi sono stati realizzati grazie alle stampanti 3D messe a disposizione dall'istituto di ricerca, e questi sono stati ottimizzati in maniera partecipativa coinvolgendo il team del Don Gnocchi e una volontaria affetta da tetraplegia incontrata tramite l'ospedale Niguarda di Milano.

Per quanto riguarda il modello finale, sono state realizzate delle simulazioni col software Abaqus/CAE per validare la scelta del materiale e, tramite ricostruzione tridimensionale dell'avambraccio di quattro collaboratori, è stato valutato il fitting del modello. È stato stampato un prototipo per uno di questi canditati sono state effettuate le prove di assemblaggio e vestibilità. Si è quindi potuto verificare che il prototipo soddisfacesse i requisiti.

Summary

Chapter 1 INTRODUCTION

1.1 Research and clinical background

In this chapter, the clinical context within which the thesis is inserted will be exposed. Information will be provided on tetraplegia and how functional electrical stimulation is helpful.

1.1.1 Spinal Cord Injury – tetraplegia

The spinal cord has segmented neurological levels that correspond to the nerve roots that exit the spinal column at the spaces between the vertebrae. There are 31 pairs of nerve roots: 8 cervical, 12 thoracic, 5 lumbar, 5 sacral and 1 coccygeal.

Symptoms of spinal cord injury (SCI) depend on the extent of the traumatic injury or non-traumatic cause, and may include sensory or motor loss of the lower limbs, trunk, and upper limbs, as well as the loss of autonomous (involuntary) adjustments of the body, the higher the injury is in the spinal cord, the more extensive the impairment. Thoracic SCI generally causes sensory and / or motor loss in the trunk and legs, called paraplegia. Lumbar SCI typically causes sensory and motor loss in the lower abdomen and legs.

Tetraplegia occurs in case of cervical spinal injuries, therefore at the level of the C1-C8 vertebrae.

In this thesis the focus will be on lesions of the C5 - C6 vertebrae, which involve total loss of mobility of the lower limbs and partial loss of mobility of the upper limbs.
All forms of SCI can also lead to chronic pain.
The global estimate of the incidence of SCI is 40–80 new cases per year per million inhabitants, based on quality studies on the incidence of all types of spinal cord injury, conducted at a national level. This means that 250,000 to 500,000 people suffer a spinal cord injury each year [1]. Cervical spinal injuries mainly affect young people, following traumatic events.
The users to whom the thesis is addressed have partial mobility that allows the extension and flexion of the wrist, with impediments at the level of the handgrip.
Paresis of the hand and upper limbs implies significant limitations to the performance of most daily activities and significantly alters the quality of life.
Physical function and independence extremely affect the quality of life (QOL) of persons with tetraplegia. Hand function was specifically identified as decreasing QOL for tetraplegic persons. This limited function had implications for writing in school and work settings, mobility in terms of opening doors and wheeling, and activities of daily living such as eating and grooming. Manns et al. [2] investigated the quality of life perceived by tetraplegic vs paraplegic persons, respondents with a tetraplegic injury stated that they frequently required adaptive equipment to compute daily living tasks and those took more time and effort than for a person with a paraplegic injury.
Optimal management of spinal cord injury rehabilitation requires a coordinated and interdisciplinary approach.

1.1.2 Traditional tetraplegia rehabilitation

Rehabilitation for patients with spinal injuries is traditionally divided into two phases: acute / subacute rehabilitation (which occurs immediately after the injury) and chronic rehabilitation (which occurs after the patient has been stabilized in the spinal unit and before to be discharged)
Most of the rehabilitation process for tetraplegics is aimed at recovering hand function, strengthening the musculature, and compensating for the imbalance of the lost muscles by seeking alternative functional responses.

The traditional approach is a necessary premise for innovative treatments. It aims to maximize motor recovery and functionality compatibly with the level of the lesion. In the tetraplegic subjects, the rehabilitation treatment is aimed at recovering the so-called "functional hand", or modifying the characteristics of the paralyzed hand in a structured and lasting way so that it can perform partial operations of gripping and releasing objects. The changes, shown in Figure 1.1, consist in shortening the tendons of the palm of the hand, so that, even if the grip muscles are deficient, the fingers can passively close following certain movements that the wrist and forearm can take thanks to their residual mobility. That of the "functional hand" is a method applied purely in the spinal units because it is more effective if started in the acute phase, immediately following the trauma.

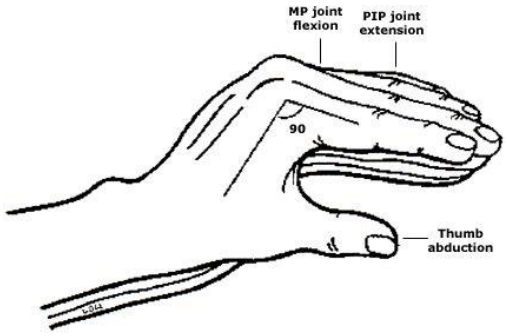

Figure 1.1 Position of functional hand. [3] Wrist in 20 to 30 degrees of extension and slight ulnal deviation, fingers in 90 degrees of Metacarpo-phalangeal joint and 15 degrees of distal interphalangeal joint and proximal interphalangeal joint, Thumb in 45 degrees of abduction.

With regard to chronic rehabilitation, a bandage is usually performed, or more rarely a customized orthosis, to keep the hand in the position that best favours grasping (dorsal extension of the wrist, dissection of the metacarpophalangeal joints, adduct and opposite thumb)

At this point the re-education process begins, during which the orthosis can be modified to optimize manual skills.

Physiotherapeutic treatments act on three fronts: with manual positioning through mobilization and stretching, with pharmaceutical treatment to prevent hypertonicity and with orthoses, which can be static or dynamic.

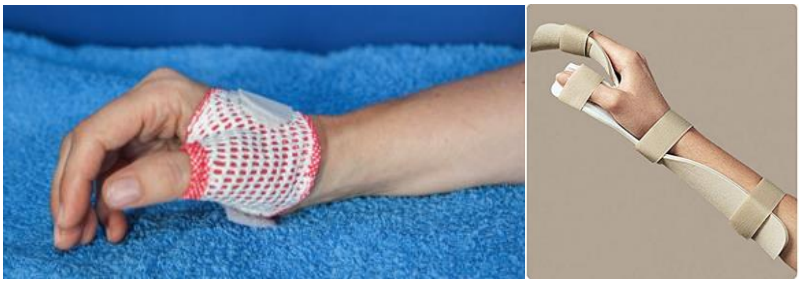

Figure 1.2 Examples of static orthoses, hand brace [4] and brace for forearm-wrist [5]. Its shown how this orthosis keeps the hand in the functional position.

Static orthoses (Figure 1.2) act on the prevention and / or correction of deformities and for joint stabilization. They can be prefabricated or made to measure and come in different materials: metals, resins, fabric, foam, etc.

Dynamic orthoses facilitate some functions by assisting or replacing muscle action. They are aimed at promoting movement, which can be carried out actively by the patient or by exploiting external forces like orthopaedic gloves that facilitates the movements of grasping of the hand supporting the extension of the fingers by elastics whose tension is adjusted according to the characteristics of the individual. An example is shown in Figure 1.3.

Figure 1.3 Example of dynamic orthosis: Saebo glove [6] commercial price of 299,00 $ USD. The tension system extends the client's fingers and thumb following grasping.

The most frequent case is that of the use of mixed orthoses, which combine static and dynamic approaches.[7] [8]

In Table 1-1 are reported the orthopaedic aid prescriptible by the Italian national health system. As can be seen in the price list, wrist-hand-finger orthoses are proposed to treat brachial plexus injury conditions, radial nerve palsy individuals who show wrist drop and / or lack of finger extension.

.

APPARECCHI ORTOPEDICI PER ARTO SUPERIORE **ISO 06.06**

DESCRIZIONE	CODICE EX D.M. 28/12/92	CODICE CLASSIFICA-ZIONE ISO	LIRE	EURO
L'applicazione e la fornitura di questi ausili è fatta dal tecnico ortopedico abilitato. Per apparecchi ortopedici dell'arto superiore si intendono le ortesi: docce, tutori.				
• **ORTESI PER MANO**		**06.06.06**		
Doccia per mano, è costituita da una doccia di alluminio plasticato o verniciato oppure di materiale sintetico; il tutto realizzato su misura da grafico e/o calco di gesso:				
- rigida	17.01.001	06.06.06.003	234.200	**120,95**
- c.s.con componenti predisposti direttamente adattati sul paziente	17.01.003	06.06.06.006	126.400	**65,28**
ORTESI PER POLSO (AVAMBRACCIO)		**06.06.09**		
Tutore per avambraccio Di acciaio inox o acciaio plastificato o verniciato o alluminio anodizzato con rivestimento in pelle o valva di stoffa o di plastica o di cuoio di contenzione dell'avambraccio. Opportune allacciature. Costruito su misura da grafico e/o da calco di gesso.				
	17.35.001	06.06.09.003	338.800	**174,98**
- c.s. con componenti predisposti direttamente adattati sul paziente	17.35.003	06.06.09.006	207.100	**106,96**
• **ORTESI PER POLSO - MANO**		**06.06.012**		
Doccia per avambraccio - mano E' costituita da una doccia di alluminio plastificato o verniciato oppure di materiale sintetico con palmare del medesimo materiale e opportune allacciature, il tutto realizzato su misura da grafico e/o calco di gesso.				
rigida c.s. con componenti predisposti direttamente sul paziente	17.05.001	06.06.12.003	288.900	**149,20**
- articolata libera	17.05.003	06.06.12.006	167.100	**86,30**
ORTESI PER POLSO - MANO - DITA	17.05.005	06.06.12.009	346.200	**178,80**
Tutore con caratteristiche dinamiche costituito da elementi predisposti da adattare sul paziente:		**06.06.13**		
- per la estensione dell'articolazione radiocarpica - per la distensione delle tre articolazioni digitali - per flessione dell'articolazione digitale media	17.31.001	06.06.13.009	110.200	**56,91**
- per flessione e contrazione flessoria dell'articolazione digitale media	17.31.003	06.06.13.012	129.200	**66,73**
- per l'estenzione dell'articolazione digitale intermedia di un dito	17.31.005	06.06.13.015	70.400	**36,36**
- per la distensione delle dita lunghe e del pollice				
- per l'estensione dell'articolazione radiocarpica e delle cinque dita (paresi del radiale)	17.31.007	06.06.13.018	72.100	**37,24**
	17.31.009	06.06.13.021	110.300	**56,97**
	17.31.011	06.06.13.024	130.600	**67,45**
	17.31.015	06.06.13.030	166.000	**85,73**

Table 1.1 list of iso classification codes of orthopaedic appliances for upper limbs from the ministry of health [9]

There is a lack of information that documents the long-term effectiveness and use of devices once the patient has returned to the community, but few studies indicate a high abandonment rate. This aspect will be deepened in the second chapter of this thesis.

1.1.3 Functional electrical stimulation

The electrical activation of the paralyzed muscle and nerve can be achieved through the use of "functional electrical stimulation" (FES), where the electrical impulse is delivered in a direct temporal relationship with the execution of the function and the user is required to “wear” the electrical device to obtain the function. Electrostimulation can have an adjuvant effect aimed at supporting or replacing functions.

Using electrostimulation, an artificial electric field is generated by means of electrodes which are applied to the skin. Under the effect of this electric field, the excitation of the nerve and muscle tissues is stimulated and the muscle contracts. Trough the electrostimulation the nerves under the lesion are stimulated in patients with damage to the upper motor neuron and directly the muscles involved in patients with damage to the lower motor neuron.

The application of the electric current to the tissue creates an action potential that propagates along the cell membrane assisted by transmembrane ion fluxes. Some tissues are more sensitive to electricity than others. The nerve membrane, for example, requires 100 times less electricity for activation than the muscle membrane. This is the reason for preferential activation of nerve or motor points and not for direct stimulation of muscle fibers to achieve muscle movement. The integrity of the anterior horn motor neuron and / or the peripheral nerve that connects to the muscle is critical. The Wallerian degeneration process (activated with the destruction of the neuronal body) produces the distal degradation of the peripheral nerve with consequent atrophy and limited ability to respond to electrical stimulation. The force of muscle contraction is controlled either by the spatial sum (by varying the amplitude or width of the electrical stimulus) or by the temporal sum (by varying the frequency of the stimulus). Physiological contraction allows for gradual control of movement by varying the number of activated muscles fibers. It also allows for efficiency as small muscle fibers, capable of sustaining prolonged activity, are recruited first. With electrical stimulation, large fibers are activated first. This allows for less modulation of the contractile force exerted by the muscles and predisposes to early-onset muscle fatigue. Due to the reproduction of the

physiological process of neuromuscular activation, electrical stimulation has found significant applications in the management of spinal cord injury.[10][11]

1.1.3.1 Rehabilitation by electrical stimulation

FES in tetraplegic patients helps restore pinch function. The best candidates are C5 - C6 level lesion patients who have preserved proximal upper limb muscle strength. The integrity of the peripheral innervation to the muscles considered for electrical stimulation is essential. These muscles should also demonstrate the ability to generate sufficient force and be resistant to fatigue.

The adaptations arising from endurance training are particularly relevant since technological devices trigger active contraction in paralyzed muscles by electrical stimulation resulting in aerobic exercise artificially performed by cycling movements of the lower limbs. In this way, we can consider that FES assisted cycling promotes a stress that can substantially modulate cellular signalling mechanisms inside paralyzed muscles resulting in adaptations to restore suitable muscle trophism, avoiding drastic and everlasting atrophy.

The interface between the stimulator and the skin is provided by electrodes. The electrodes must be biocompatible, safe, have appropriate longevity, and provide sufficient selectivity to guaranty that only the targeted motor system is activated.

The current technology allows the use of basically any shape of electrodes with many small pads (area approximately 1 cm^2) and the conductive gel. Sensors made with micro- and nano-technology can be used in FES systems for real-time monitoring of position, velocity, acceleration, orientation in space, distance, and many other physical properties. The current sensors are small, require low energy and can be integrated with a microcomputer and wireless communication circuitry. The therapeutic use of FES is benefiting from the new array electrodes and effective stimulators, particularly when integrated with exercises to provide excitation feedback [11]–[18][19]–[22]

1.1.4 Forearm anatomy

Since the objective of the thesis is to design an orthosis that is positioned on the forearm and electrically stimulates some muscles to restore the grip of the hand, in this chapter will be exposed the range of motion we want to preserve and the muscular anatomy.

The anterior forearm muscles provide for wrist and finger flexion, forearm pronation, wrist adduction, and wrist abduction.

The posterior forearm muscles, on the other hand, control the extension of the wrist and fingers of the hand, supination of the forearm, flexion of the elbow, the extension of the elbow, and abduction of the thumb.

A necessary parameter for the design of the orthosis will be to preserve the pronation and adduction movements of the forearm, and to allow the positioning of the electrode for the stimulation on the flexors muscle and the recording electrodes on the extensors muscles as illustrated in Figure 1.4.

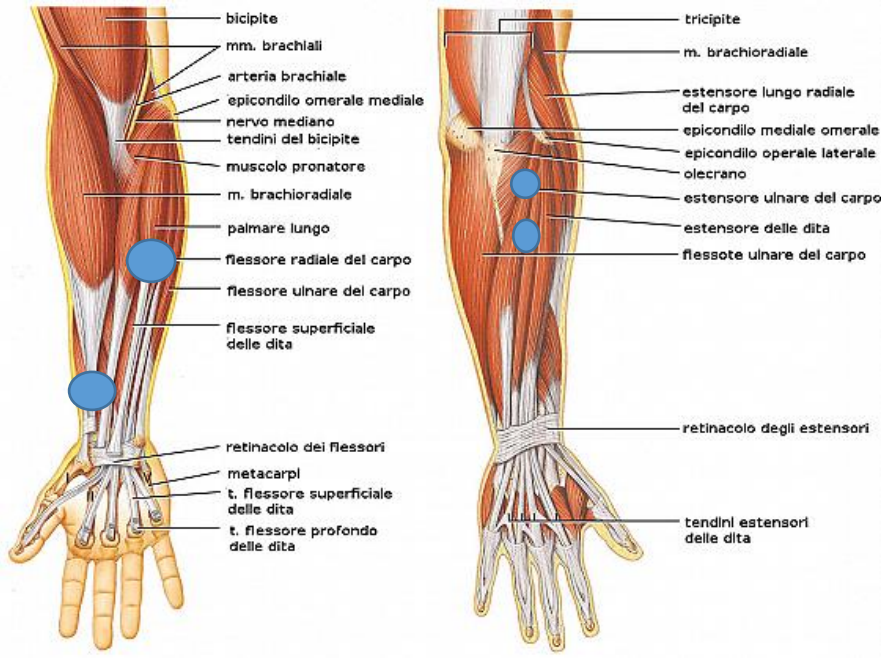

Figure 1.4 Position of the forearm prone and abducted and its muscles [6]. The circles identify approximately the estimated position of the electrodes, in the image on the left those for stimulation, in the one on the right those for recording

1.2 Objectives

The use of functional electrical stimulation not only in the rehabilitation field but also in the home context is of growing interest. Starting from the work of engineer Thorsen, a researcher at the Don Gnocchi Institute in Milan, who developed a myoelectric controlled electrostimulator (MeCFES), the aim of this thesis is to make this technology affordable for people with chronic diseases, not with the intent of a functional recovery but as an assistance in carrying out daily activities, creating an orthosis that can help the user to wear the MeCFES independently. This thesis addresses tetraplegic subjects with residual mobility in the upper limbs, with the hope of being able to restore their independence.

The decision tree that led to the design of the prototype will be illustrated. This will be validated by performing computational tests to verify its resistance and functionality.

The orthosis will be made directly achievable by the user, do-it-yourself (DIY) and tailor-made, therefore fitting tests will be performed through 3D reconstruction of the anatomical component, to verify that the dimensions of the prototype fit correctly.

A simulation of the 3D printing and assembly of the final prototype will be reported to be compared with the computational data obtained for validation.

Finally, a study will be carried out on the manufacturing costs in comparison with the devices currently on the market.

Chapter 2 STATE OF THE ART

This chapter will illustrate the state of the art regarding wearable devices on the market that use the FES and will be explained the operation of the MeCFES device, developed by Eng. Thorsen. The theme of open source and co-design will then be explored in the context of assistive devices by investigating the involvement of users both in the design and the production of the devices themselves.
The rapid prototyping techniques used in the thesis and the materials used will be illustrated, ad it will be explained how to 3D reconstruct anthropometric data thanks to new smartphone scan technology.

2.1 FES devices for hand rehabilitation on the market

There are presented the devices on the market that use functional electrical stimulation for hand rehabilitation. These devices are for clinical use, therefore designed for rehabilitation sessions and not for daily and autonomous use.

1. The H200 Wireless Hand Rehabilitation System

Figure 2.1 The H200 Wireless Hand Rehabilitation System; [21] It is composed of a forearm-wrist brace, integrated by a 5-channel FES system for the activation of the flexors and extensors of the wrist / fingers and of the thumb muscles allowing the individual to grasp and release objects.

The H200 Wireless Hand Rehabilitation System (Figure 2.1) supports the wrist in a functioning position, allowing the fingers and thumb to move efficiently while reaching, grasping and pinching.

The H200 consists of an orthosis and its control unit. The control unit transmits synchronous electrical impulses to the peripheral nerves through electrodes located in the orthosis. These activate five muscle groups of the forearm and hand: extensor digitorum, extensor pollicis brevis, flexor digitorum superficialis, flexor pollicis longus, thenar group. Designed to provide a proper set of impulse in synchronized muscle functional activity. The orthosis fits to the forearm and wrist and communicates wirelessly with the control unit. Inside the orthosis, electrodes deliver mild stimulation that helps the hand move.

The hand-held remote-control unit lets the user adjust the level of stimulation and turn the unit on and off.

There are flexible and modular components to optimize the fit and maintain optimal contact with the electrodes. The positioning of the electrodes can be changed by means of the clinical electrode location system. The intensity of the stimulation can be modulated. Stimulation is activated with manual control of a keypad that communicates wirelessly with the orthosis.

The device is therefore optimal for the rehabilitation of subjects suffering from hemiparesis, therefore able to operate the control unit or assisted by a physician. Some possible benefits includes the improvement of voluntary movements and functional abilities, reduction of muscle spasm, increase or maintenance of range of motion improvement in local blood circulation and postpone disuse atrophy.

It is not an aid device that can be used autonomously by tetraplegic subjects to perform daily actions, as the stimulation must be activated manually from the control unit, but it provides a good example of a modular orthosis that can be adapted to the user's needs.

The commercial price ranges between 3000 and 5000 $ USD, hence it is a substantial expense to be incurred for a private individual.

2. The OmniHi5™ Advanced FES Upper Extremity Treatment System

Figure 2.2 The OmniHi5™ Advanced FES Upper Extremity Treatment System [23] is a wearable functional electrical stimulation (FES) system for the upper limb which, thanks to an integrated electromyographic sensor, is activated by the intended movement of the user.

The OmniHi5™ (Figure 2.2) is designed to provide electrical stimulation for patient who are experiencing upper limb paralysis or paresis. The closer it is placed to the wrist the more it provides finger extension, the further away it is from the wrist the more it involves wrist extension. It has a screen and a built-in control unit. It has different modes, to meet specific need of the patient and can be used both as rehabilitation therapy and assistive device. It is provided with build in metal electrodes for the stimulation and can be used alone or controlled via app.

It is possible to connect it with hydrogels electrodes (Figure 2.3), to be applied on wet skin to increase conduction. In this mode, the device can record the EMG from the muscle on which the hydrogel electrodes are placed that derives from the intention of movement, and activate a proportional electrical stimulation to assist the movement intended.

Figure 2.3 OmniHi5™ placement of hydrogel electrodes to use EMG control of FES.

The muscle contraction is activated by the voluntary intention of the movement, OmniHi5™ detects signals from the muscles to use as a guide, delivering the amount of stimulation necessary to assist with moving the wrist, hand, and fingers. This teaches the brain a new pattern of movement.

It is applied to the wet forearm with a Velcro band. The intensity of the stimulation is displayed wirelessly via tablet and is variable. It adapts to patient-specific needs, incorporates engaging exercise visualizations, and enables therapeutic protocols in rehab and functional capabilities outside of rehab to enhance independence and quality of life. It is designed to improve hand function and active range of motion in patients with hemiplegia or upper limb paralysis. The application of the device cannot be performed autonomously by a tetraplegic user but it can be extremely helpful in assisting everyday tasks.

It is indicated for Maintenance or increase of ROM, reduce muscle spasms, prevent or delay inactivity atrophy, promote neuromuscular re-education and recovery.

This device is available for purchase only in Australia and is on hold for FDA (Food and Drug Administration) approbation to be commercialised in the US (phase II).

The information about its price found so far indicates a cost of 3500 euros for its purchase.

2.2 MeCFES

From the examples given above, both for static or dynamic orthotics and for electrostimulators on the market, it can be seen that there is no device that deals with hand grip rehabilitation for people with tetraplegia to be used independently. It is therefore in this context that the MeCFES fits in. MeCFES is a neuroprosthesis capable of enhancing functional activity thanks to the interface between the machine and the nervous system, it uses functional electrical stimulation with myoelectric control. The principle of working is that the residual electromyographic (EMG) activity of a partially paralysed muscle, still under voluntary control, can be used to control the electrical stimulation of the same or other synergic muscles. It requires 5 surface electrodes placed on the skin above the muscle. The electrodes are two stimulation electrodes, two recording electrodes and one for active electrical ground. From the recorded signal the device will estimate the voluntary activity of the muscle. This estimate controls the amplitude of the stimulation. The user thus controls

the stimulation intensity by the voluntary contraction of the controlled muscle [12], [13]. The device use is for recovering the hand grip of persons affected by lesions of the Central Nervous System.

In the case of tetraplegic users, the EMG signal is detected from muscles controlling the extension of wrist and fingers by superficial recording electrodes, then it is processed and used to stimulate the target muscles, the fingers flexors, through stimulation electrodes. The principle on which MeCFES is based is reinforcement of the tenodesis mechanism: it consists in the passive flexion of fingers due to wrist extension. Thus, the patient himself can drive the neuroprosthesis through his voluntary muscle contraction.

Figure 2.4 . The tenodesis grip. The left figure shows the relaxed position of the hand with the wrist in flexion, on the right side is show the extension of the wrist with the consequently enclosure of the fingers

If the passive mechanical tenodesis properties are adequate, this grip is used as follows: with the wrist in flexion, the fingers are manipulated around a target (a object to be held). Then the wrist is actively extended, causing passive finger flexion and the target can then be held. In Figure 2.4 the tenodesis grip is shown: in the left the wrist is in flexion, so the fingers can enclose the target; in the right (Figure 2.4) the wrist is extended, causing passive finger flexion, so the target can be held. The stimulation level is directly proportional to the amplitude of the EMG signal that is detected from recording electrodes. Thus, stimulation amplitude is computed as a function of the myoelectric level. The function limits the stimulation to a maximum current amplitude to avoid overstimulation. A consequence of this “proportional” and continuous control of FES is that the subject must sustain activation of the controlling muscle to maintain a stimulation output. The simulation signal is defined by threshold, Gain, and maximal stimulation. These

parameters are user defined by an android application connected via Bluetooth to the system (interface shown in figure 2.5).

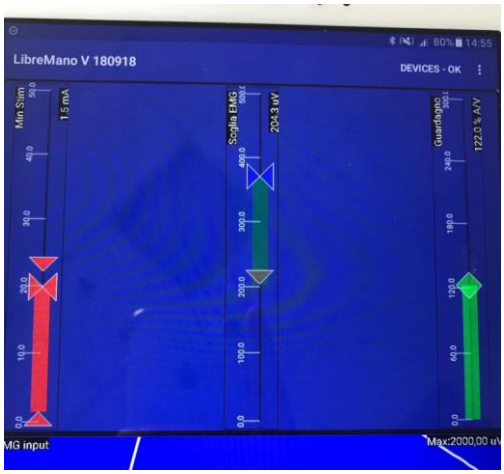

Figure 2.5 Application interface. the slider on the right modulates Gain, the one in the center the amplitude of the stimulation and the one on the left limits the maximum stimulation. the EMG of the recorded signal is shown below

The stimulation consisted of biphasic 300 µs rectangular impulses with a 300 µs interphase interval and a 16.6 pulses per second fixed repetition rate. The dimension of the device is 11 × 3 × 6 cm with a weight of 200 g and it is powered by two rechargeable 1.5 V AA type batteries. Standard surface self-adhesive stimulation electrodes (Figure 2.6) and EMG recording electrodes are used and connected to the MeCFES unit by flexible cables.

Figure 2.6 Electrode positioning for MeCFES. On the left is shown the positioning of the electrodes for the stimulation, on the right the positioning of the recording electrodes.

As for the electrical stimulation, this takes place on the lower side of the forearm. In particular, the stimulation electrodes are positioned near the flexor muscles of the fingers (FDP = flexor digitorum profundus, FDS = flexor digitorum superficialis, FPL = flexor pollicis longus) while those for detecting the myoelectric signal on the extensor radialis muscle of the carpus, the ECR (ECR = extensor carpi radialis longus / brevis) distal to the

radiohumeral joint . The recording electrodes are placed longitudinally to the long axis of the muscle aligned in the direction of the fibers.
[23]–[25] .
Currently the MeCFES is in experimental phase in the clinical setting at the Don Gnocchi Foundation for rehabilitation sessions, it will be examined in depth during the thesis how the system has been studied to make it a home assistance device

2.3 Customized rehabilitation devices / Co-design

Mass-produced assistive devices do not always fit patient-specific needs. This leads to an often underestimated problem of abandonment and inactivity. Garber et al. [1] studied the extent to which tetraplegic patients used and were satisfied with various types of devices, one and two years after their first rehabilitation experience
The devices were either commercially available, therapist-adapted and therapist-fabricated, or orthotist constructed. The population studied consisted of 56 subjects with spinal cord injury resulting in tetraplegia. Spinal cord-injury levels ranged from C2 to T1, 66% of the subjects had lesions between C5 and C7. Descriptive data were obtained regarding the prescribed upper extremity assistive devices.
The results of this study show how 54% of the device prescribed were in use after 1 year. This percentage decrease to 35% at the end of the second year in analysis.
As for the issue in assistive devices (AD) of the abandonment or non-use, some of the reasons pointed out as responsible for these phenomena are lack of fitness, high costs and stigma. Today, there are 600 million people living with disabilities who lack proper assistive devices or whose AD does not yet fit well [27]. As patients may not give feedback on reasons for abandonment to the provider, the AD designs may suffer from lack of development and adaptation to the users specific needs .The solution may be to involve the patient directly in the design and production of her/his personal AD since disabled people are often outstanding problem solvers because they simply have to be creative. Life for disabled people is a continuous series of challenges to be overcome. This is the case when therapists are creating or customizing ADs for their clients in the orthopaedic workshop. [28][29]–[31]

Disabled users and their caregivers have a high incentive to make, adapt or create new AD and improvements in technology allows to produce unique assistive devices fabricated with rapid manufacturing tools and standard resources. [27]

In this case we speak of Co-Design, and this process involves three main figures, schematised in Figure 2.7:

- The occupational therapist, who detects which type of assistive device the patient needs to achieve his or her goals, and by doing so sets the starting point for the first design, or customisation iterations. therapist evaluates the flow experienced in every iteration through the behaviour and feedback of the patient.

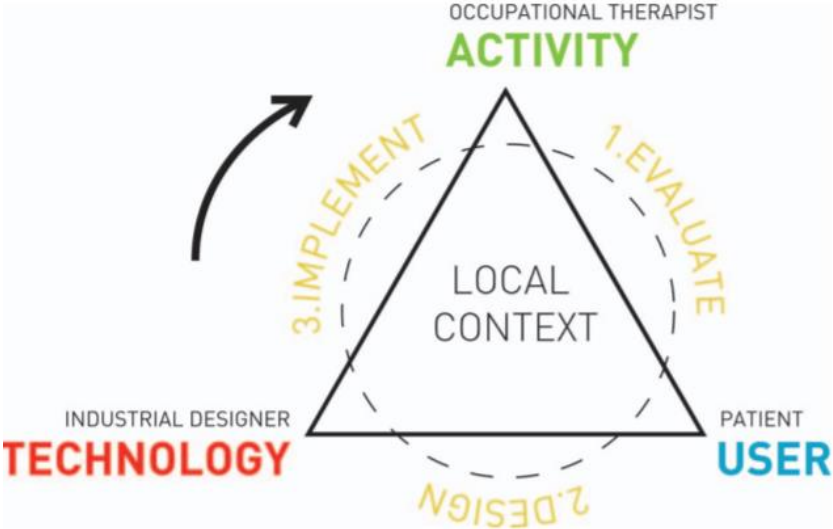

Figure 2.7 scheme of the co-design decision-making process, which connects the user with the designer and the therapist in a cyclical way. [26]

- The patient, who is given the position of 'expert of his/her experience'. He or she seeks assistance in fulfilling a meaningful goal. In some cases,
  when the patient has difficulty communicating his or her feedback verbally, the caretaker plays an important role as translator.
- The industrial designers, who becomes the technology facilitator between the occupational therapist and the patient. They continuously translate user values and feedback through behaviour into product properties. With this human-centred design approach, the designers try to augment the skills and ability of the patient through adapting the technology.

Johnston et al. [32] investigated how assistive devices obtained involving the patient leads to creating something that they actually need, and a percentage of participants that continued using their technology was reported to be very high.

2.3.1 Rehabilitation devices tailored/ Do it yourself

Thanks to digital fabrication (DF), it opens the possibility of creating tailor-made and do-it-yourself rehabilitation devices. Digital fabrication is part of a broader horizon and of a technological and social movement such as that of Makers, digital artisans. It consists in the possibility of building three-dimensional solid objects by oneself, through digital drawings, whether they are finished objects, study models, models, or prototypes. The movement of open source from software also extends to free hardware, making some technologies accessible to mass users to produce products of many types on their own, in a domestic dimension, in a small company or within a FabLab.

Portnova et al. [33] describe how their digitally fabricated hand orthoses shows promise as a cost-effective alternative to off-the-shelf and custom-fit metal devices.

Innovative manufacturing techniques such as 3D printing, whose operation will be deepened in the next chapter, for customizable and user-specific hardware has led to open-source Do It Yourself "DIY" production of assistive devices, having an incredible impact globally for families with little recourse.

As advancements in DF make prototyping of mechanical parts and electronic devices available and affordable, people with special needs may start to 'homebrew' AD solutions.

By Manero et al. [34] is reported how the outlook for using 3D printing manufacturing techniques and collaborative design is bright, with rapidly progressing iteration and designs that can better develop affinities for users. A good example of how to reconcile digital manufacturing and the concept of open source with the creation of customized and do-it-yourself prostheses is that offered by the platform e-NABLE [35], that is an online global community of "Digital Humanitarian" volunteers from all over the world who are using their 3D printers to make free or low-cost prosthetic upper limb devices for children and adults in need. The open-source designs created by e-NABLE Volunteers help those who were born

or lost their fingers. Provides a design catalogue with free access, including an instruction manual for construction and assembly of the device. It connects those who need this type of prosthesis with those who can 3D print the components and sells DIY kits for their realization.

2.4 3D printing

Rapid prototyping (RP) is a technology that allows the production of objects with complex geometry, in a very short time, starting from the mathematical definition made on a three-dimensional CAD model end slicing it into sections of infinitesimal thickness.
prototype is thus created section by section, transforming the problem from three-dimensional to two-dimensional. The objects are obtained with the progressive addition of matter. For this reason, RP technology is also defined as a production technique by layers or by floors.
In this thesis, 3D printers that use the Fused deposition modelling (FDM) printing process will be used. In the FDM process, an extrusion head moves on a table in two main directions: a thermoplastic filament is melted inside an extrusion head and then extruded through a small opening on the printing plate. The initial layer is placed on the printing plate, while the subsequent layers are obtained with the same procedure, lowering the plate, deposed one over the other.
The design phases consist of creating the model using CAD design software, exporting the model in the form of a .stl file, using a software to perform slicing and exporting the g-code for the 3D printer. [25] - [31]
In this thesis the prototype was designed through the Onshape Edu online platform which allows students access to every tool for design and editing of shared document via cloud services. This option has favoured a collaborative design process.
As for the 3D printers were used the following:

- The Olivetti s2 printer (Figure 2.8), with two extruders and compatible with filaments with a diameter of 1.75mm. It has a direct printing mode, characterized by the positioning of the extruder motor directly above the hot end. As slicer software was

used the Silc3rPE-1.42.0-alpha5 + win64 to generate the g-code compatible with the Olivetti printer.

Figure 2.8 Olivetti s2 printer [36]. Above the printer are visible the extruders inside which the filament will be iserted. the print bed is in the rest position and will move closer to the extruders during printing

- The Ultimaker s5 printer (Figure 2.9) , with two extruders and compatible with filaments with a diameter of 2.85mm. It has a Bowden printing mode where the extruder motor is mounted on the frame, pushing the filament through a PTFE tube towards the hot end. As slicer software was used the Ultimaker's Cura 4.2.0 to generate the g-code compatible with the Ultimaker printer.

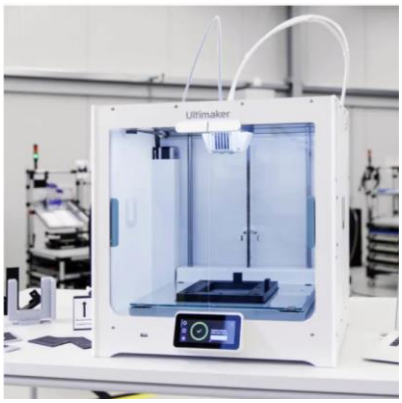

Figure 2.9 Ultimaker s5 [37]. Above the printer is visible the tube for the filament extrusion at the end of which there are the extruders. the print bed is in the rest position and will move closer to the extruders during printing

2.4.1 Printing Materials

In this paragraph will be listed the mechanical characteristics of the materials that were used for the printing of the prototypes during this thesis. The materials are presented in the form of filaments, rolled up in coil and inserted into the printer nozzles (Figure 2.10)

Figure 2.10 PLA coil [38]

- Polylactic acid (PLA): it is a bioplastic as it is derived from the fermentation of corn. The relationship between stress and deformations is reported in (figure 2.11) (it has a modulus of young E = 3500MPa.
  It can be printed at relatively low temperatures, between 170 ° and 210 °.
  It has excellent adhesion to the printing surface which therefore does not necessarily have to be heated. It can be printed at high speeds up to 60mm / s.
  It is therefore an excellent material to use for rapid prototyping as it is easy to print and low cost (300g x € 14.96 [39]). It does not have high mechanical characteristics.

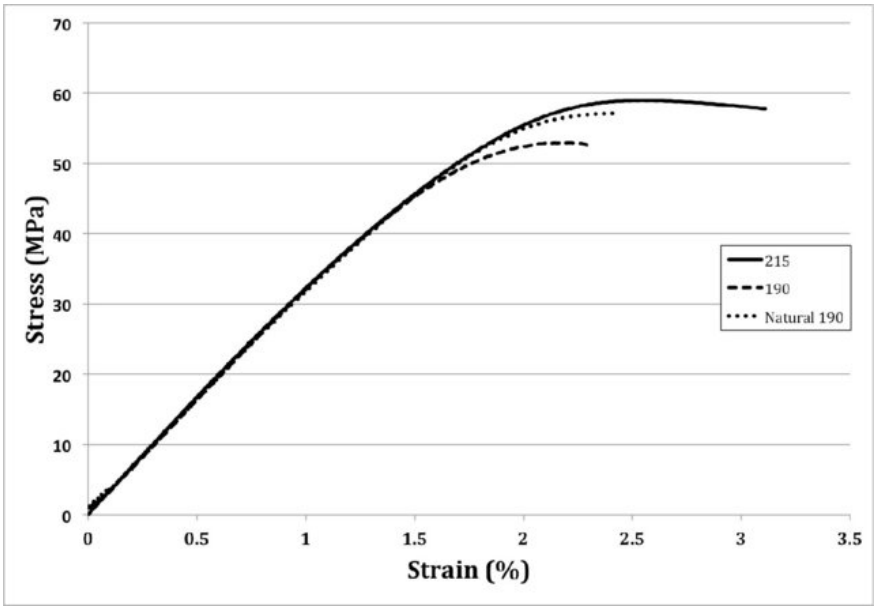

Figure 2.11 stress vs strain curve for PLA [40]. it has an elastic phase for deformations up to 1.5% and subsequently a plastic phase for deformations up to 2.5% after which the material undergoes breakage

- Polyvinyl Acetate (PVA): it is a water-soluble material. It is used in FDM processes as a support for other materials, to then be dissolved in water. It has printing characteristics comparable to PLA. It has a higher cost than PLA (500g x 51,13euro [41]) but its use rarely, just for printing complex geometries supports.

- FilaFlex, is a thermoplastic elastomer (TPE). In the case of TPE the printing temperature is much higher than that of PLA and is covered between 220° and 260°. It has an elastic modulus E = 95 Mpa and its main characteristic concerns its high flexibility. The recommended print speed is around 30mm/s and it costs € 44.50 per 500g spool [42]

- Thermoplastic Polyurethane (TPU). Two TPUs were used in the thesis, the first for printing with Olivetti (Ninjaflex, filament diameter 1.75mm) the second for printing with Ultimaker (TPU95A, filament diameter 2.85mm. As for the TPE it was choose for its high flexibility.

Since this is the material with which the final prototype was made and on which the computational analyses were carried out, its characterization will be further explored below.

2.4.1.1 Hyperelastic material characterization

The computational tests were carried out on the Abaqus / CAE software. To simulate the behaviour of the TPU material, an incompressible isotropic hyperelastic model was chosen. A certainly relevant and complete study in this area is that of Shahzad et al. [43] where suitable hyperelastic methods and models of Strain Energy Function (SEF) for the characterization of rubber are analysed. Experimental data from the literature were used [43] and it was possible to compare the different models and by fitting the experimental curves to ascertain which was the ideal model to predict the behaviour of the rubber under consideration.

Monotonic tensile tests were performed by Major et al. [44] from loading rates of 1 to100 mm/s and at test temperatures -40°C, 23 °C and 50 °C to characterize the large strain monotonic deformation behaviour of thermoplastic polyurethanes (TPU) using both flat and cylindrical specimens. Examples of stress strain curves for TPU are shown in Figure 2.12 at -40, 23 and 50 °C and at loading rates of 1, 10 and 100 mm/s.

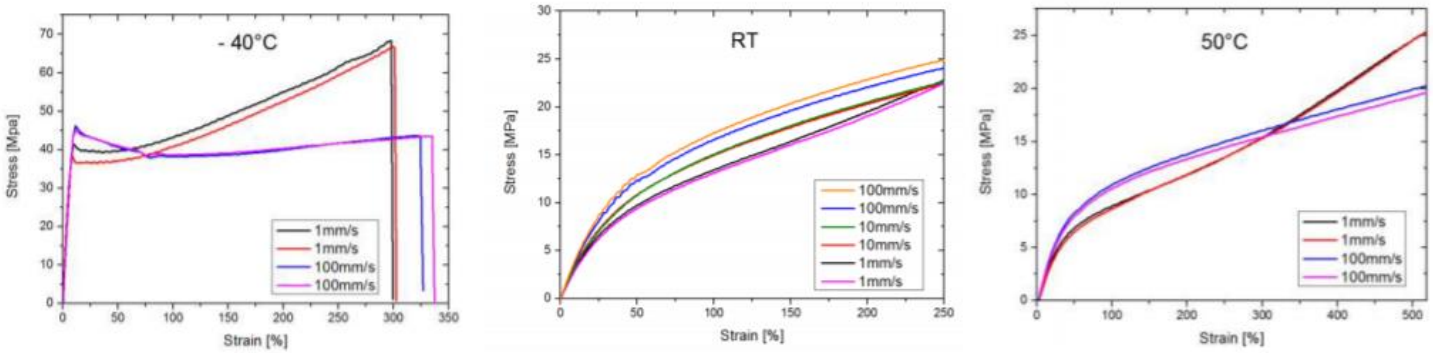

Figure 2.12 Stress Strain curves for TPU performed by Major et al. The curves are plotted for different temperature and loading rates.

The large strain deformation behaviour reveals different temperature dependence for the TPU. For the purpose of this thesis the room temperature (RT) curves (Figure 2.13) was taken into consideration.

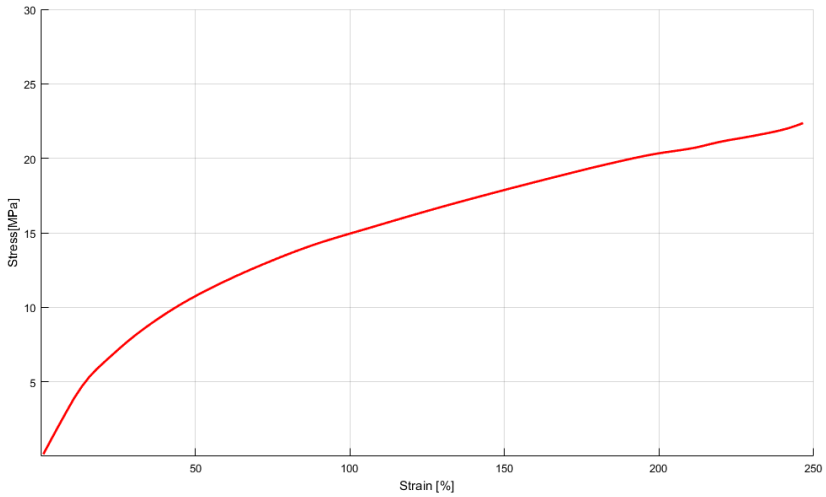

Figure 2.13 Stress stran curve at room temperature. Is visible how the material il deformable up to 250 % under stress between 20 and 25 MPa.

In the paper is also reported the long-term failure behaviour, characterized by Wöhler curves. Displacement controlled tensile fatigue tests were carried out using a diabolo-type specimen configuration at various temperatures and at both low and high frequencies. TPU is considered to be a rubber like material and its ability to withstand very large strains without permanent deformation or fracture makes it ideal for many applications. The traditional approach in rubber fatigue models for predicting fatigue life in rubber focuses on predicting crack nucleation life, given the history of quantities that are defined at a material point, in the sense of continuum mechanics. Stress and strain are examples of such quantities. Strain is a natural choice because it can be directly determined from displacements, which can be readily measured in rubber. The results of uniaxial fatigue are mostly related with maximum principal strain. [45]

Major et al. generated local strain based Wöhler curves by using the hysteretic curves, the Fmax/Fmin values and the cycle number-to-failure, Nf as reported il Figure 2.14.

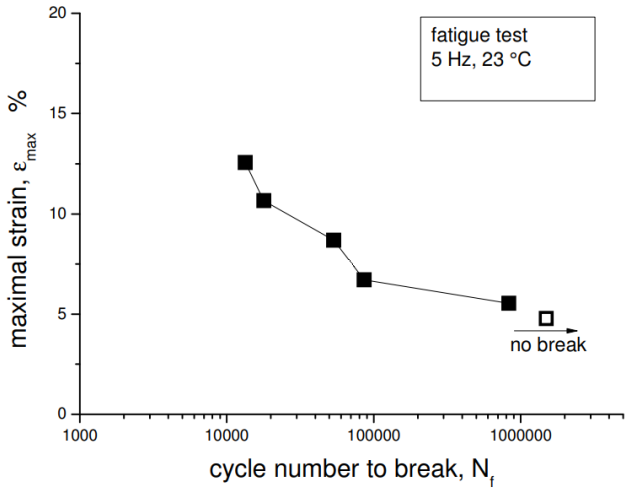

Figure 2.14 Woler strain based fatigue curve performed by Major et al. shows the maximum deformations that the material can withstand without breaking as the number of load cycles varies.

As in this thesis were performed fatigue consideration on the TPU behaviour, the previous curve was used as a comparison.

2.5 3D reconstruction

Industrial 3D measurement systems have reached a state of development where a multitude of different measurement tasks can be accomplished with precision and at high speed. However, systems with these features are expensive and difficult to access. In 2010 Microsoft launched the Kinect system with the "Xbox 360" game console that works according to the time-of-flight method, to estimate in real time the distance between the camera and the framed objects or scene, measuring the time it takes a light pulse to travel the camera-object-camera path.

In the fall of 2018, Apple released the iPhone X, a smartphone capable of providing 3D data thanks to the TrueDepth sensor system based on the principle of structured light.

The functionality of the camera system is comparable to that of Microsoft's Kinect camera system. A point projector projects more than 30,000 dots onto a surface in front of the device. The infrared camera then receives the reflection of these light points and can create a surface model from the resulting model. To ensure accurate detection even in low light conditions,

the system is supported by an infrared radiator, which also illuminates the area in front of the camera.

The TrueDepth system first uses the Flood illuminator to irradiate the light and infrared to establish the presence of a face, then the Dot projector to flash 30,000 points on the surface of the object and finally the infrared camera to read the data.

The main function of the TrueDepth camera is facial recognition but this system is used by various apps for scanning three-dimensional objects.

The iPhone X's TrueDepth system can be used to measure activity with millimeter accuracy. Further confirmation on the accuracy of the TrueDepth iPhone X camera system is provided by Alfaro-Santafè et al. [47] which illustrates the use of this device for foot scanning and demonstrates its excellent reliability in the measurements. It also shows how these measurements can be used for the anthropometric classification, as will be done in this thesis.

Chapter 3 MATERIALS AND METHODS

The device that was designed during this project aims to improve the grasping capabilities of people with tetraplegia. Specifically, it's an assistive aid that can be placed on the forearm. The design is conceived to be participative: it means that the final user was actively involved as a participant in the design and creation phase.

The device incorporates a novel technology for using myoelectrical controlled functional electrical stimulation (MeCFES).

It consists in a "cage" integrated with electrodes that detect a myoelectrical signal originated by the extension of the wrist and consequently electrically stimulates the muscles to obtain finger flexion.

In this chapter the decision-making process that led to the construction of the final prototype of the electrode applicator will be explained.

The components are: electrodes, MeCFES, power supply and electrodes applicator.

Since this is an assistive device for chronic condition, the intent is that the user is able to wear and remove it independently and to keep it worn all day. The strengths consist in creating a connection as involvement with the user, since his role doesn't consist in being treated passively but better in actively taking part in both the design and the assembly of the device. The final product will indeed be built by the user since he is provided with instructions that gives the information necessary to personalize your anthropometric data, print and assemble the whole device. It's believed that involving the user is helpful in understanding the problem that each of them individually face daily, to adapt and optimize the product and it's thought that this approach could also help the user in accepting and feeling confident with the device itself.

Another fundamental aspect lies in the affordability of the product since the materials used are mostly TPU (for the 3D printing of the cage), disposable electrodes and the MeCFES electronic card, the costs of which are lower compared with preassembled devices on the market.

3.1 Electrodes

To transmit the myoelectric signals from the muscle to the amplifier and the stimulation current to the muscle, surface electrodes are used. There are some general requirements that the electrodes must fulfil and when stimulation and recording is performed in the same area extra constraints apply to the electrodes.

The electrodes should have the following properties:

• A good electrical contact to the skin

• Low impedance

• Biocompatibility, i.e. cause no skin irritations during long term use

• Easy to apply.

A choice of 30mm in diameter is be regarded safe. The electrodes must ensure good uniform skin contact. In theory, the stimulation should be applied where the nerve enters the muscle or over the endplate zone of the muscle.

The electrodes are coated with a conductive gel that makes them adhesive. For the purpose of the project, a layer of synthetic deerskin was interposed between the adhesive surface of the electrodes and the skin, making these reusable.

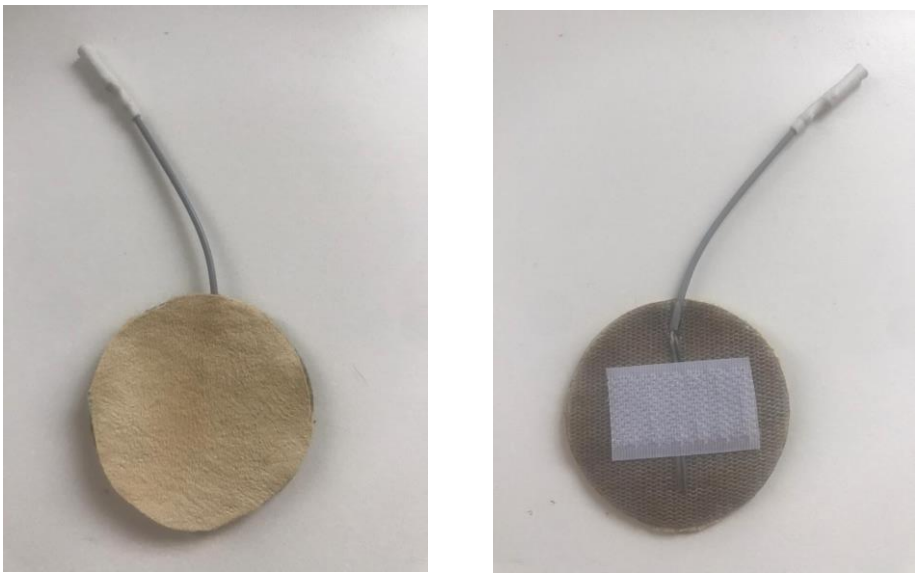

Figure 3.1 Electrode for stimulation coated with synthetic deerskin and adhesive velcro on the back to provide fixation on the electrode applicator.

Synthetic deerskin was experimentally proven to be conductive, and its conductibility increases if wet.

Due to the stochastic nature of the myoelectrical signal it is believed that it is not easy to filter out the motion artefacts. For this reason, the electrodes must be protected from mechanical influences and stretching of the skin must be avoided.

3.2 Electrodes Applicator

The prototypes developed process wanted to meet the following requirements:

- Optimal fit, to keep the electrodes firmly in position in contact with the arm, to optimize the conduction of stimulation and avoid motion artefacts.
- Support the physiological movements of the forearm, especially pronation and supination.
- Comfortable, to be worn daily.
- Easily worn independently by the user.
- Do-it-yourself.
- Low cost

The design was made using the open source OnShape CAD drawing program.

All the measures have been defined as parametrical, hence the design is customizable automatically by inputting the user measurements.

```
FeatureScript 1024;
import(path : "onshape/std/geometry.fs", version : "1024.0");

const VALUES = { // Below we have the global variables for the antropometrical measurements
    "wristheight" : 40* millimeter,
    "armlength" : 230* millimeter,
    "DPWidth" : 60 * millimeter,     //Width of the wrist
    "DPDiam" : 65* millimeter,     //Height of the wrist

    "DPRadius" : 10 * millimeter,     //Radius of curvature of the wrist
    "PPDiam" : 95 * millimeter,
    "PPCircumference"  : 268 * millimeter,
    "fattoredimodifica": 0* millimeter // rispetto ad armlenth di 220mm

};
annotation { "Feature Type Name" : "Arm measurements" }
export const setGlobals = defineFeature(function(context is Context, id is Id, definition is map)
    precondition
    {
    }
    {
        for (var value in VALUES)
            setVariable(context, value.key, value.value);
    });
```

Figure 3.2 Script parametric anatomical measurement Onshape

```
FeatureScript 1024;
import(path : "onshape/std/geometry.fs", version : "1024.0");

const VALUES = { // Below we have the global variables driving the design:
    "thickness" : 2.1 * millimeter,
    "connhole" : 2.2 * millimeter,   //Connector hole
    "bandwidth" : 20 * millimeter,  //The width of the wrist band
    "padding": 2 * millimeter,
    "distanzabuco": 10 * millimeter,
    "bandasottile" : 1 * millimeter,
    "distanzaxbottone" : 3 * millimeter,
    "distanzaybottone" : 4 * millimeter,
};
annotation { "Feature Type Name" : "Global Dimensions" }
export const setGlobals = defineFeature(function(context is Context, id is Id, definition is map)
    precondition
    {
    }
    {
        for (var value in VALUES)
            setVariable(context, value.key, value.value);
    });
```

Figure 3.3 Script dimension parameter Onshape

In fact, it is sufficient to replace the numerical values and the whole drawing automatically adapts to the change.

The measurements to size the parts were taken at the proximal end of the ulna (For convenience, it is measured up to where the elbow bends) and at the head of the ulna or radius (Distal circumference, wrist circumference). The measurements were the width of the wrist and forearm taken manually with a calibre, with the subject's arm resting prone on a plane. The length of the forearm was measured between the wrist and the proximal end of the ulna as shown in Figure 3.4.

Figure 3.4 Positioning of the caliber to extract anthropometric measurements.

3.2.1 Evolution of the prototype

3.2.1.1 First Prototype

The first approach was to make two rigid bracelets to be placed at the wrist and below the elbow.

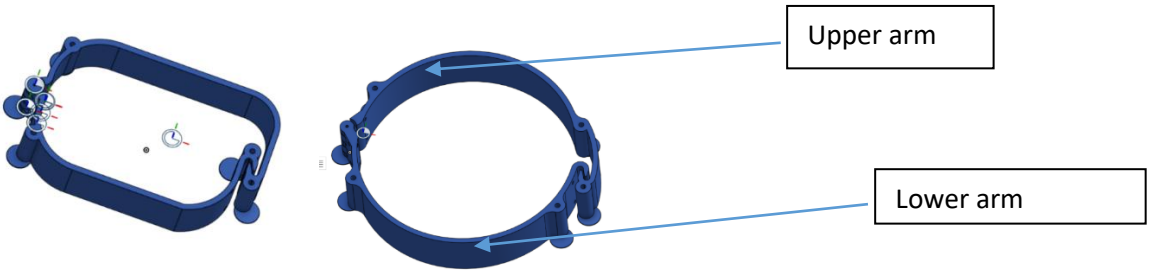

Figure 3.5 wrist bracelet and elbow bracelet (the circles at the base are used in the printing phase to better adhere the structure to the printing surface, they have the same height as the first layer and are easily removable during assembly.

The bracelets open with a zipper and close with hooks. Polylactic acid (PLA 3D print filament 1.75mm) was chosen as printing material.

The idea of this type of closure lies in the misalignment between the upper and lower arm of the bracelets: by imposing a pressure on the upper arm of the bracelet, it slides over the lower one and overcomes it. Releasing this pressure the upper arm of the bracelet will tend to return to the rest position, but it will interlock with the hook of the lower arm. On the contrary, to open it, its necessary to apply a new pressure on the upper arm and shift slightly in a radial direction to release the joint.

To connect the two bracelets and thus create a cage to support the electrodes, thermoplastic elastomer (TPE) FilaFlex bars were made, this being a material with high flexibility to accommodate the physiological movements of the arm.

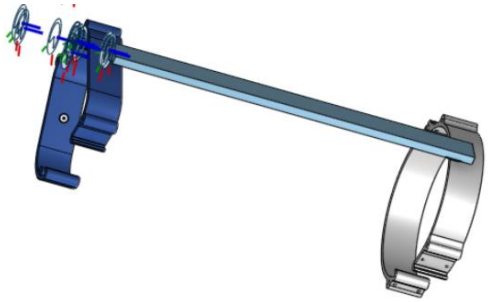

Figure 3.6 FilaFlex flexible bar connecting the wrist and elbow bracelets.

The slicing was done with Silc3rPE-1.42.0-alpha5 + win64 software with a printing temperature of 180 degrees and printing speed of 50 mm / s for the PLA and printing temperature of 240 degrees, bed temperature of 30 degrees and printing speed of 15 mm/s for the TPE.

Another parameter to take into account when printing is that of the infill, or the percentage of filling, of the object. This also changes the mechanical properties of the printed object compared to those of the material. By reducing the thread, flexibility will be increased and vice versa. During the various printing tests, variable infills were tested, evaluating the results obtained qualitatively. Since this parameter also influences the printing speed (more material to extrude more time to extrude it) in the field of prototyping was always tried to minimize it, net of the mechanical characteristics.

The assembly of the bracelets with the bars was done with screws. Velcro bands were then sewn across the bars as buttonholes, so that were movable along the length of the device, on which the electrodes were hooked in order to position them in the most appropriate location to optimize stimulation and detection of the myoelectric signal.

The print was made with the Olivetti s2 printer. The final assembly is shown in Figure 3.7 in closed configuration and in Figure 3.8 in open configuration.

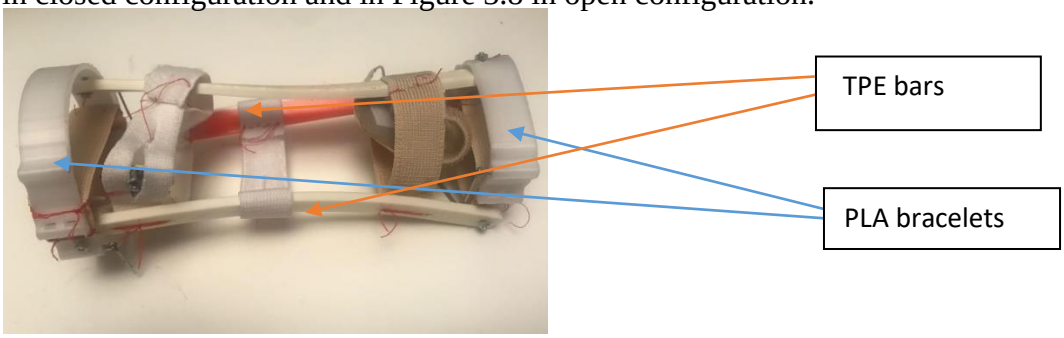

Figure 3.7 First Prototype assembly in close configuration. Shows the PLA brachalets, the TPE bars and the Velcro bands

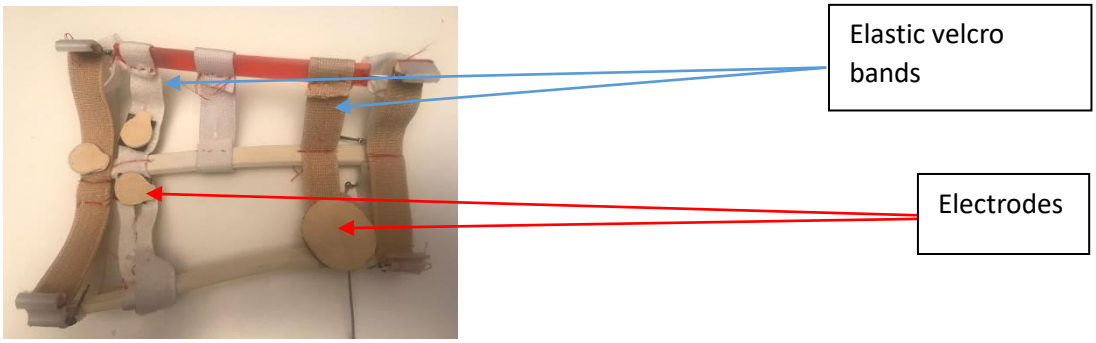

Figure 3.8 First prototype in open configuration. It shows the positioning of the electrodes un the Velcro bands.

This prototype does not take into account the allocation of the electronics yet. In Figure 3.9 its show the prototype worn and how it allows different movements of the forearm.

Figure 3.9 First prototype worn, it's shown the range of motion allowed by the prototype. A collaborator was asked to wear the device, perform prono-supination, grasp a bottle and approach it to the mouth by flexing the elbow

3.2.1.2 Co design experience at Niguarda hospital

This first prototype was subjected to evaluation by Alessandra, a young girl suffering from tetraplegia, who kindly made herself available to participate in the project, thanks to the cooperation of the Niguarda Hospital team.

After a first phase of positioning the electrodes (Figure 3.10) and calibrating the stimulation intensity, the electrodes were positioned on the first prototype and the participant was asked to wear the device independently.

Qualitative grasp tests were carried out on various objects and the comfort of the orthosis was evaluated.

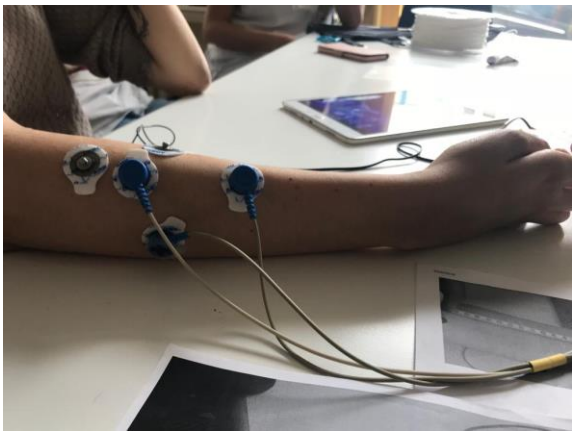

Figure 3.10 Electrode placement on Alessandra on the extensor muscles of the forearm to detect the electromyographic signal and calibrate the MeCFES

Following the Co-design process illustrated by De Couvreur et al. [27] The occupational therapist role was occupied by the Niguarda team, who proposed ideas taken from the world of physiotherapy such as the use of Velcro bandages with a ring for closing.

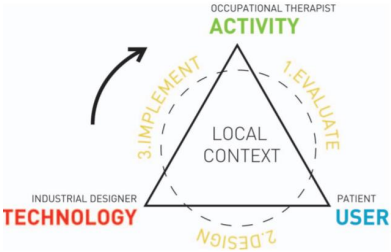

Figure 3.11 Scheme of the co-design decision-making process, which connects the user with the designer and the therapist in a cyclical way. [[26]

Alessandra, as user, has held the role of 'expert of her experience' giving feedback on her feelings in using the prototype. The designer, we of the Don Gnocchi team, joined as technology facilitators between the occupational therapist and the user by translating values and feedback through behaviour into product properties.

The considerations made through this process are summarized in the following table:

Requirements	First Prototype
Optimal fit	So and so The bracelets and bars are adaptable to the user's measurements The movable Velcro straps allow you to place the electrodes in a different position but not all anatomical points of interest are reachable

Support the physiological movements of the forearm	So and so The TPE bars have a good flexibility but are bound too rigidly to the bracelets so the movements are difficult
Comfortable	So and so The Velcro bands interposed between the structure and the arm offer good comfort but the bracelets on the wrist does not fit comfortably
Easily worn independently by the user	No The TPE bars make the structure too instable, it cannot be closed with a single fluid movement
Do-it-yourself	So and so Feasible, but it involves several assembly steps including sewing the Velcro bands.
Low cost	Ok The material used and the realisation technique allow to produce the device affordably

Table 3.1 Project requirement for the first prototype

After evaluating the characteristics of the prototype with Alessandra and the Niguarda team, we discussed possible improvements and changes to be made.

3.2.1.3 Second Prototype

Thanks to Alessandra's participation, a second version of the prototype was therefore created:
to maximize the surface on which to apply the electrodes to ensure maximum adaptability inter users, a grid (Figure 3.12) in TPU thermoplastic polyurethane (NinjaFlex 3D-Print Filament - 1.75mm) was created.

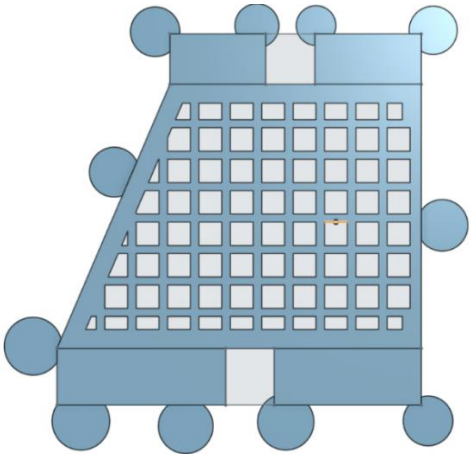

Figure 3.12 Printing design of the flexible grid. the rectangles at the upper and lower ends are half a millimeter thick to be pierced and fix the grid to the PLA components. The circles are used to fix the structure during printing and are 0.2 mm thick

The wrist bracelet design (Figure 3.13) was modified to make it more comfortable and anatomically compatible, while keeping PLA as the material.

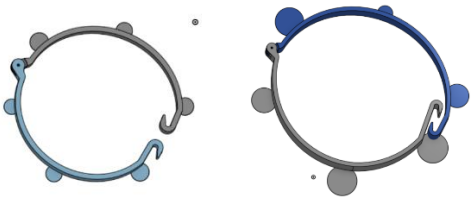

Figure 3.13 The wrist bracelet design has a oval conformation with respect to the previous design (left image) wile the elbow bracelet has been slightly flated (right image).

The same closure of the bracelets was maintained and a Velcro closure was added along the length of the grid to keep it firmly adherent to the arm during the twists.
The slicing was made with the Silc3rPE-1.42.0-alpha5 + win64 software, and the print was made with the Olivetti s2 3D printer

The assembly between the grid and the bracelets was carried out by drilling the ends of the grid and the bracelets and tying them with cable ties. The final assembly is shown in Figure 3.14.

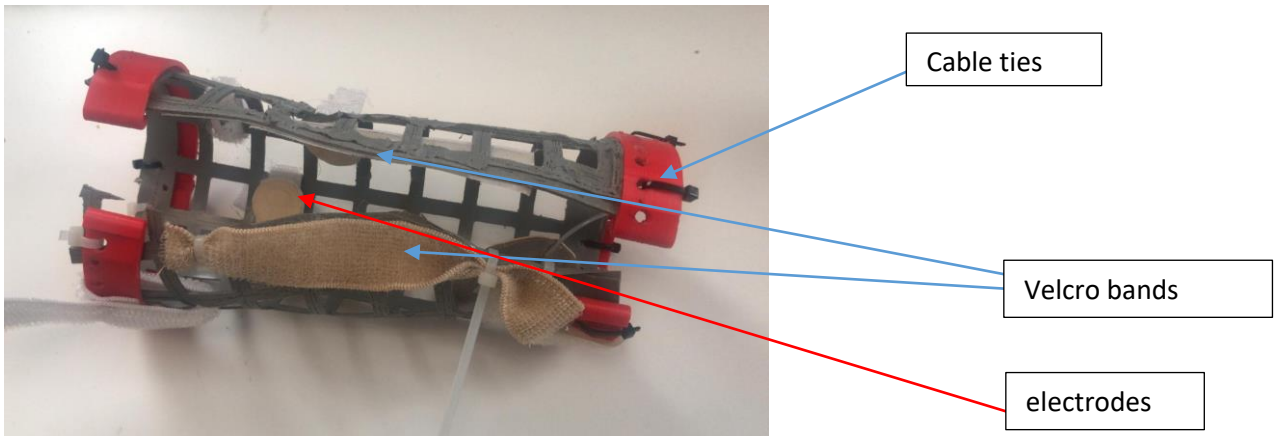

Figure 3.14 Second Prototipe assembly. It shows the placement of the electrodes and the fixation of the TPU grid with the PLA bracelets by cable ties.

3.2.1.4 Co design experience at Meet me tonight

During the development of the thesis, I had the opportunity to participate, together with the research department of the Don Gnocchi Foundation, at "La note dei Ricercatori, Meet me tonight", a scientific dissemination event in the gardens of Porta Venezia in Milan with the theme "Personalized Medicine" On the 28th of September 2019.

A stand was dedicated to the foundation Don Gnocchi IRCCS and Engineer Thorsen invited me to present the second prototype to the public. There was therefore an opportunity to test the electrode applicator on a large number of participants and collect feedback.

The assessments made during the event are collected in the following table:

Requirements	Second Prototype
Optimal fit	Ok The bracelets and bars are adaptable to the user's measurements

	The grid allows you to freely position the electrodes ensuring the achievement of the optimal position for stimulation.
Support the physiological movements of the forearm	Ok The TPU grid allows an optimal range of movement and thanks to the Velcro closure ensures excellent adherence between electrodes and skin during physiological movements.
Comfortable	So and so The PLA bracelets stiffen the structure making it uncomfortable during accentuated wrist or elbow flexions
Easily worn independently by the user	No The hooks of the bracelets are not very smooth in the closing phase and tend to unhook during too accentuated twisting of the forearm. The Velcro used for closing the flexible component is too strong and makes it difficult to remove the device
Do-it-yourself	So and so Feasible, but it involves several assembly steps including fastening the Velcro bands and cable ties.

Low cost	Ok The material used and the realisation technique allow to produce the device affordably

Table 3.2 Project requirement for the second prototype

Also in this case, the allocation of the MeCFES was not considered in the assembly. In Figure 3.15 its show the prototipe worn and how it allows different movements of the forearm.

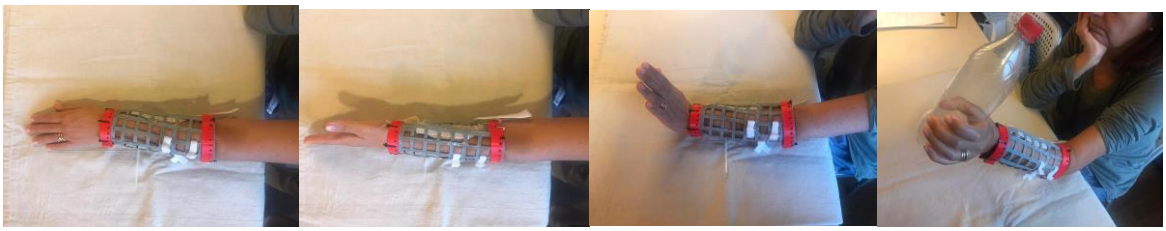

Figure 3.15 Fitting of the second prototype. A collaborator was asked to wear the device, perform prono-supination, grasp a bottle and approach it to the mouth by flexing the elbow

3.2.1.5 Final Prototype

With the purchase by the Don Gnocchi Foundation of the new Ultimaker s5 3D printer, the possibility of creating more complex designs has opened. Wanting to reduce the final assembly phase as much as possible, it was decided to create a cage (Figure 3.16) to be printed as a single piece, entirely in TPU (TPU95A Ultimaker) by making a printing support in polyvinyl alcohol (PVA), a water-soluble filament. The drawing was also built in a parametric way in order to make it adaptable by modifying single variables. The thickness of the electrodes to be interposed between the prototype and the forearm was considered.

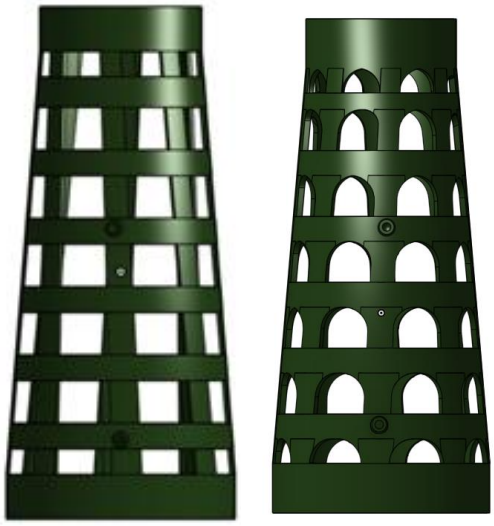

Figure 3.16 model of th TPU cage. On the right is represented the original model and on the left il shown the arched configuration of the lateral openings.

To minimize the consumption of the support material, and therefore reduce both printing times and costs, the side openings have been joined in an arched configuration (Figure 3.17), so as not to create the so-called bridges: these are extruded layers " in the void ". In Figure 3.17 it is easy to see how this leads to structural failure.

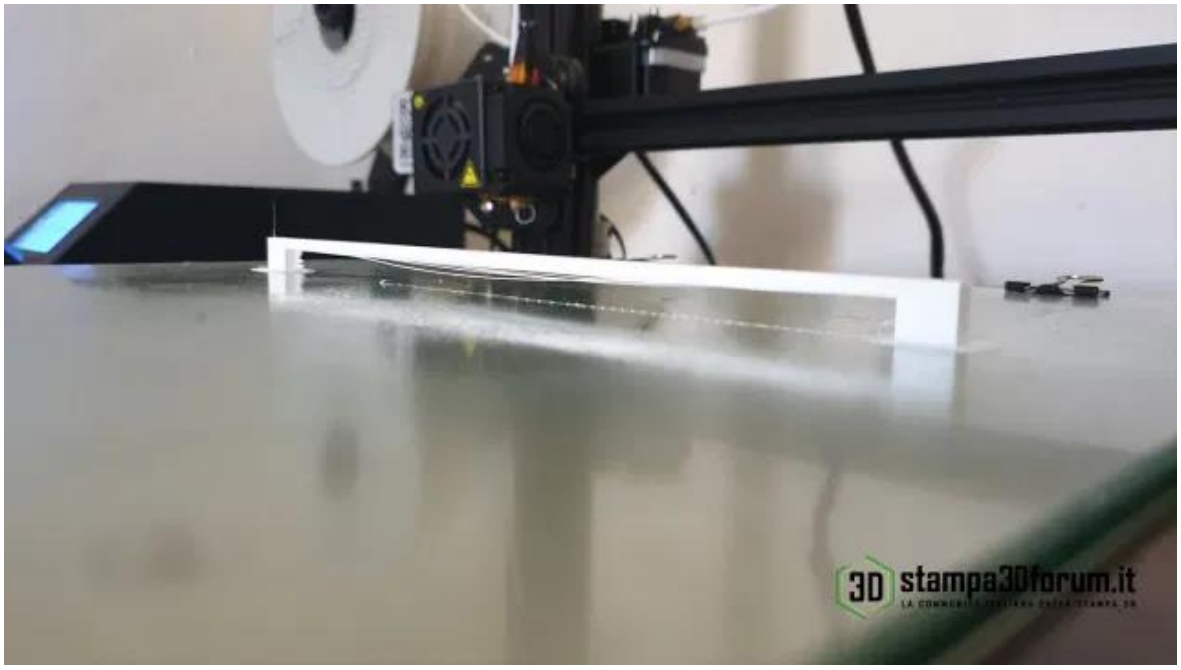

Figure 3.17 [48] Its shown the bridge problem of printing. The first layer extruded in the void collapses.

By maintaining rectangular openings, it would have been necessary to introduce the PVA support along the entire structure (Figure 3.18).

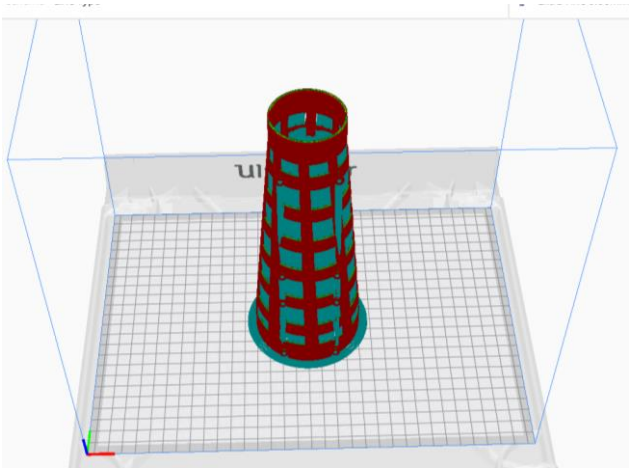

Figure 3.18 Printing setup. red part corresponds to the TPU structure, the blue part represents the PVA support created by the software automatically to avoid structure failure during the printing

With the arch configuration the consumption of the product is considerably reduced and Printing times are reduced from 4 days to 24 hours! A further positive consequence was the reduction in the price. By making online quotes on sites that offer the printing service, this is reduced from 150 euros to 50 euros. The printing parameters used are:
Layer height 0.2 mm
Extrusion temperature: 230 degrees
Floor temperature 60 degrees
Extrusion speed 30 mm / sec

The rigid components of the PLA bracelets were therefore eliminated. The closure was made with Velcro bands for physiotherapeutic use. To allow opening and closure of the device, a connection band was prepared between the upper and lower part of the device with a lower thickness, to ensure maximum flexibility. The allocation of the box with the electronic components and one for the removable and rechargeable battery was obtained by preparing bases in which to insert automatic buttons (Figure 3.19) available in an haberdashery (this aspect will be better explained later in the paragraph describing the assembly. The characteristics of the design are shown in Appendix A.

Figure 3.19 Automatic buttons with external

diameter of 10 mm and internal on 4,6 mm

The battery box (Figure 3.21) was made on the model of the battery of a BlackBerry Curve 8520 device (Figure 3.20), having a removable connector and battery and given its easy availability on the market. (also this aspect will be better treated in the assembly paragraph)

Figure 3.20 BlackBerry Curve 8520, used to extract the battery and connector

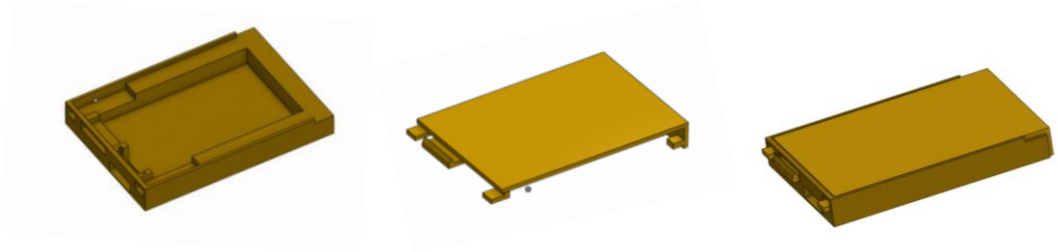

Figure 3.21 Battery box with removable lid design, made to allow the extraction of the rechargeable battery.

As for the electronics box, a normal electronic board size box was created with holes at the apexes to be screwed (Figure 3.22)

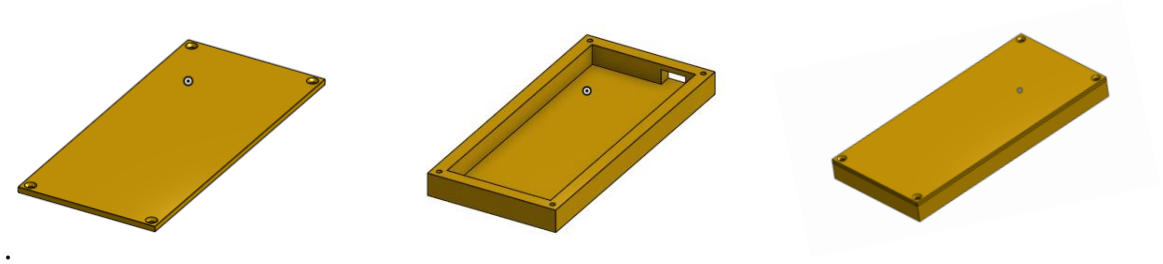

.

Figure 3.22 Electronic box with screw-on lid.

The characteristics of the design are shown in Appendix B.

The materials with which the latter were made is Tough PLA.

In this case, printing is much faster as the geometry is simpler, and PLA is a printable material at higher speeds. By making online quotes on sites that offer the printing service, the estimated price is around 15 euros per component

The printing parameters used are:

Layer height 0.2 mm

Extrusion temperature: 180 degrees

Floor temperature: 30 degrees

Extrusion speed: 60 mm / sec

In Figure 3.24 is show the assebly between the TPU cage and the electronic and battery boxes.

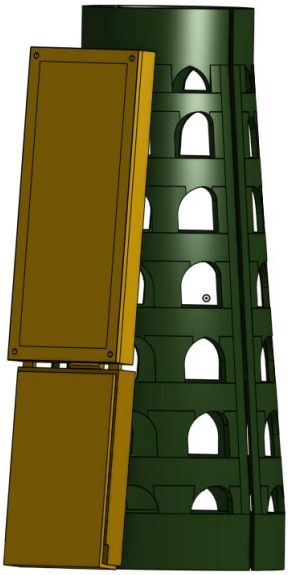

Figure 3.23 Assembly of the cage with the electronic, realized with the assembly tool in Onshape

Below are the instructions for making the device:

1. Sizing:
   - Sign up for free on OnShape
   - Access the following link:
     https://cad.onshape.com/documents/ddee4543490719265e825328/w/69eef7f23294fb22d837e91c/e/3a000f454d09236e20e26f7d
     the following page will open

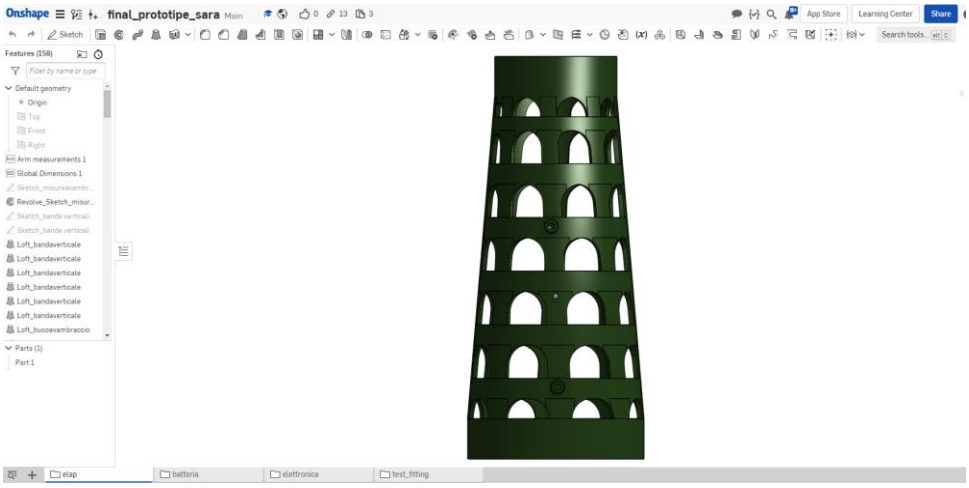

- Go to the “elap” folder (standing for electrode applicator)
- Enter the "antrodata" page.

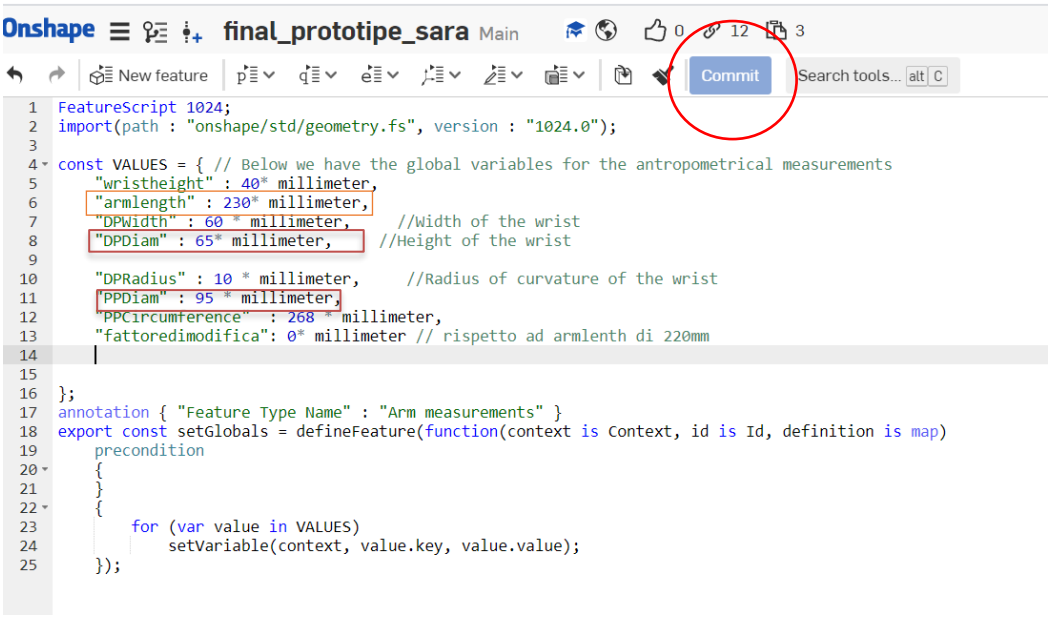

- Modify the parameters "armlenght" with the length in millimetres of your forearm, "DPDiam" with the width of your wrist in millimetres and "PPDiam" with the width in millimetres of the forearm measured below the edge (as described at the beginning of chapter 3) and select "commit" at the top right. At this point the drawing will adapt to the measures entered.

2. Data export:
   - Right click on the “3D model” window and select export.

- Enter the following parameters and give the ok to save the .stl file

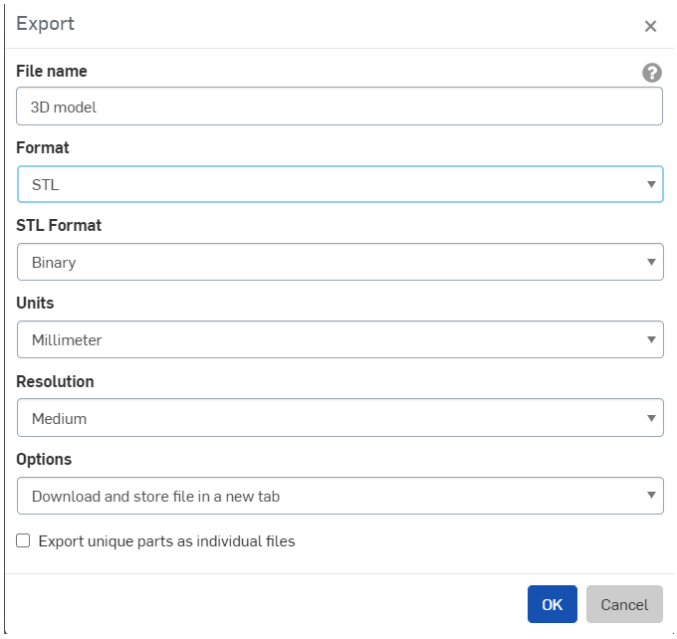

- Click on the window with the house icon
- Enter the "batteria" folder and perform the same operation to export the “boxbatteria" and "coperchiobatteria" files
- Enter the "electronica" folder and perform the same operation to export the "box-elettronica" and "coperchio-elettronica" files

3. Print:

At this point you can send the files to an online printing service which will proceed with the printing of the various components, if you are equipped with a 3D printer you can proceed with the slicing and the creation of the g-code to be sent to your printer or you can print it yourself in a FabLab with the expertise support of their staff.

Reminder that the prototype was analysed for TPU materials and the boxes for electronic components in tough PLA, in case you want to use other materials it will be up to the user to adapt the printing parameters to the specific case.

4. Assembly

For assembly, the following tools are needed:

- The 3D printed components
- Velcro band for medical use

- 2 plastic rings (e.g. shower curtain rings)
- 2 snap buttons (external diameter 10 mm internal diameter 4.6 mm)
- 1 BlackBerry Curve 8520 (also damaged but with working battery)
- Hot glue or Attack
- 4 self-tapping screws (size)
- Screwdriver
- Stapler
- Scissors

dismember the BlackBerry Curve 8520, extract the connector (sliding removal) and insert the latter in the appropriate seat in the battery box

Figure 3.24 Battery box assembly process. From the first image on the top left there's the BlackBerry dismembered, the connector extracted, the connector placed on its seat in the battery box, the battery placed in it seat in the battery box, the lid in open configuration and the lid in closed configuration

Insert the battery and close the lid by sliding it over the base, exerting a slight pressure to allow the interlocking (to open it, press and slide it in the opposite direction) as shoun in Figure 3.26.

For the electronics box, just screw the 4 screws at the corners of the lid. With hot glue, glue the female component of the buttons in the appropriate seat on the TPU cage. Glue the male component of the buttons to the center of the boxes for the battery and electronics (Figure 3.27).

Figure 3.25 Assembly the electronic box with the TPU cage. From the left image there is the placement of the female part of the botton in its seat (of a TPU printing test), the male part of the botton placed in the center of the electronics box, the box assembled on the TPU part of the old prototipe.

Cut the Velcro band of the desired length and fix it on the outer ends of the cage with the stapler (Figure 3.28).

Figure 3.26 Test to evaluate the possibility to fix the Velcro band on the TPU part with the stapler.

To help in closing and opening the prototype, plastic rings can be attached to the Velcro band, so that the tetraplegic user can insert his fingers and close the cage (Figure 3.29).

Figure 3.27 Ideal result of the plastic ring assembly, shown on a commercial wrist orthosis [49]

It will therefore be possible to purchase the electronic components including cables to connect the electrodes and the electrodes themselves.

At this point, together with a physiatrist, it will be possible to establish the optimal position of the electrodes and then fix them, with Velcro, to the cage. The last aspect will be to calibrate the optimal electrical stimulation via the app (figure 3.31).

Figure 3.28 Experimental testing for calibration performed on a healthy subject.

Once ready, it will be possible for the tetraplegic subject to wear the applicator independently, which will then hold the electrodes firmly in the optimal position to allow stimulation (to assist in closing the hand) whenever necessary during the day.

3.2.1.6 **Final prototype experimental tests**

The final prototype was printed (Figure 3.29), sized on a healthy collaborator to verify correct fit and ease of assembly. The tests conducted were to carry out the assembly of the various components as described in the previous chapter and to verify that the correct positioning of the electrodes was allowed referring to photos taken during the calibration phase of the MeCFES on the subject (Figure 3.29).

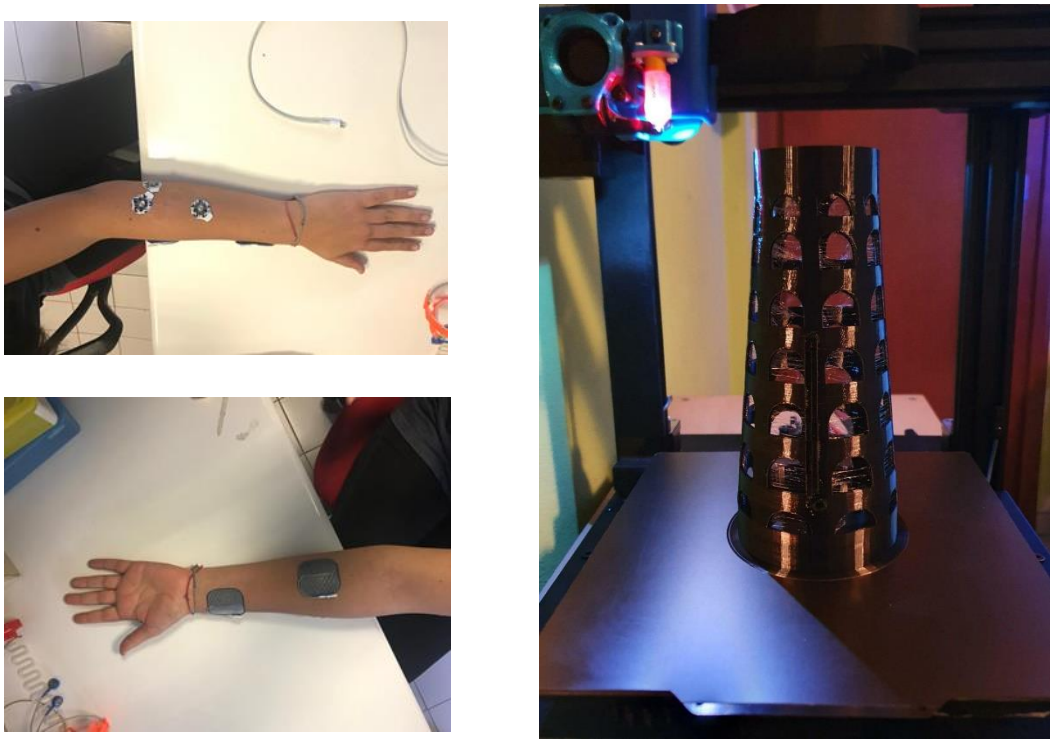

Figure 3.29 on the left its shown the placement of the recording electrodes (longitudinally placed on the extensor muscle of the forearm plus the ground) and the stimulation electrodes (placed on the flexors muscles). On the right the finished prototype in the printer.

3.3 Fatigue analysis

To confirm that the choice of material was in accordance with the needs, it was decided to carry out numerical simulations using the Abaqus CAE software.

The simulations are aimed at verifying the resistance of the chosen material, in particular the fatigue resistance was evaluated in the most loaded point, which was found as expected in the cage connection band. The opening of the device was simulated, and the results were compared with the data relating to the mechanical fatigue of the TPU reported in the literature.

3.3.1 Characterization of the material

In order to proceed with the computational simulation, is necessary to characterize the material (i.e. choose the most appropriate model of the Strain Energy Function and determine

its characteristic coefficients). Biaxial experimental were obtained from the stress vs strain graphs reported in the literature, using MATLAB

```
[filename, pathname] = uigetfile('*.PNG','Select the image file:');
nomefile=strcat(pathname,filename);
image=imread(nomefile);
hfig=figure;
him=imshow(image,[]);
hsp=imscrollpanel(hfig,him);
apisp=iptgetapi(hsp);
h=msgbox('Seleziona l''origine del sistema di riferimento.');
waitfor(h);
[x0,y0,P0] = impixel;
h=msgbox('Seleziona il punto finale dell''asse x.');
waitfor(h);
[x1,y1,P1] = impixel;
h=msgbox('Seleziona il punto finale dell''asse y.');
waitfor(h);
[x2,y2,P2] = impixel;
h=msgbox('Scegli i punti sulla curva.');
waitfor(h);
[xi,yi,Pi] = impixel;
% trasliamo tutto sull'origine
xn=xi-x0;
yn=y0-yi;
m1=(y1-y0)/(x1-x0);
m2=(x2-x0)/(y0-y2);
xrot=xn-yn*m1;
yrot=yn+xn*m2;
prompt={'Qual è il massimo valore della grandezza sull''asse x?'};
titolo='Ampiezza intervallo x.';
numlines=1;
defaultanswer={'0'};
answer=inputdlg(prompt,titolo,numlines,defaultanswer);
deltax=str2double(cell2mat(answer(1,1)));
prompt={'Qual è il massimo valore della grandezza sull''asse y?'};
titolo='Ampiezza intervallo y.';
numlines=1;
defaultanswer={'0'};
answer=inputdlg(prompt,titolo,numlines,defaultanswer);
deltay=str2double(cell2mat(answer(1,1)));
x=xrot.*(deltax/(sqrt((x1-x0)^2+(y1-y0)^2)));
y=yrot.*(deltay/(sqrt((x2-x0)^2+(y2-y0)^2)));
close all;
figure;
hold on;
plot(x,y,'-b');
set(gca,'xlim',[0 deltax],'ylim',[0 deltay]);
t=linspace(min(x),max(x),100);
p=pchip(x,y,t);
plot(t,p,'-r');
t=t';
p=p';
A = [t, p];
```

Figure 3.30 Script from Professor Votta exam Advanced modelling approach for cardiovascular surgery by Marco Stevanella

with those predicted by the hyperelastic model it is possible to obtain the values of the coefficients of the model by minimizing the squared deviations between the two, this part will be dealt with later in the part concerning the fitting of the Parameters.

3.3.1.1 Fitting hyperelastic model

The choice of hyperelastic models fell on those that are already implemented in the Abaqus software, whose Strain Energy Function assumes the incompressibility of the material (J = 1) in this form:

- Neo-Hookean, $W_{NH} = c_{10}(\bar{I}_1 - 3)$

- Mooney-Rivilin, $W_{MR} = c_{10}(\bar{I}_1 - 3) + c_{01}(\bar{I}_2 - 3) +$
- Yeoh, $W_Y = c_{10}(\bar{I}_1 - 3) + c_{20}(\bar{I}_1 - 3)^2 + c_{20}(\bar{I}_1 - 3)^3$
- Ogden, $W_O = \frac{2\mu}{\alpha^2}\left(\bar{\lambda}_1^{\alpha} + \bar{\lambda}_1^{\alpha} + \bar{\lambda}_1^{\alpha} - 3\right)$

where λ are the principal stretch ratios from the strain gradient tensor, and I are the invariants of the Cauchy-Green tensor, referring to Abaqus user manual 19.5.1 [50]
By replacing the stretch ratio data obtained from the graph of the experimental tests, the values of nominal stresses predicted by each hyperelastic model dependent on the respective coefficients are obtained.$(c_{10}, c_{01} \ldots \alpha, \mu)$.

3.3.2 Abaqus CAE simulation

To determine the optimal coefficient values, a fitting was carried out directly on Abaqus by importing the test data into the edit material window. At this point the evaluate function was activated in the "material manager" which outputs the stress strain curves approximated by the models (Figure 3.31)

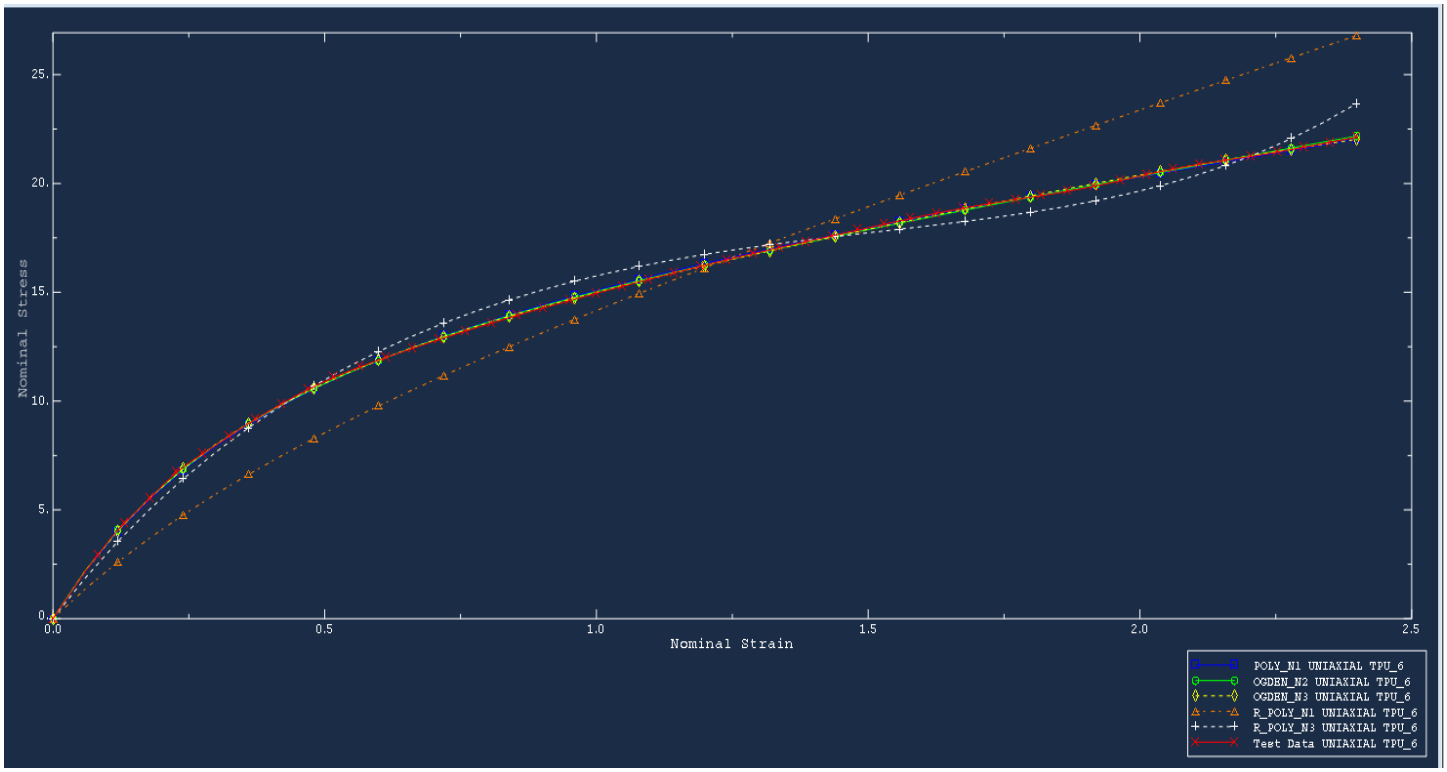

Figure 3.31 Fitting hyperelastic models. POLY_N1 (Mooney-Rivlin) in blue , ODGEN_N2 in green , ODGEN_N3 in yellow , R_POLY_N1(Neo-Hook) in orange ,R_POLY_N3 (Yeoh) in withe, Test Data in red.

From the graph it was assessed that the best fitting was obtained by the Ogden model of polynomial order 2 and 3 since they minimized the root mean square error (RMSE). Abaqus returns the coefficients to enter to use this model

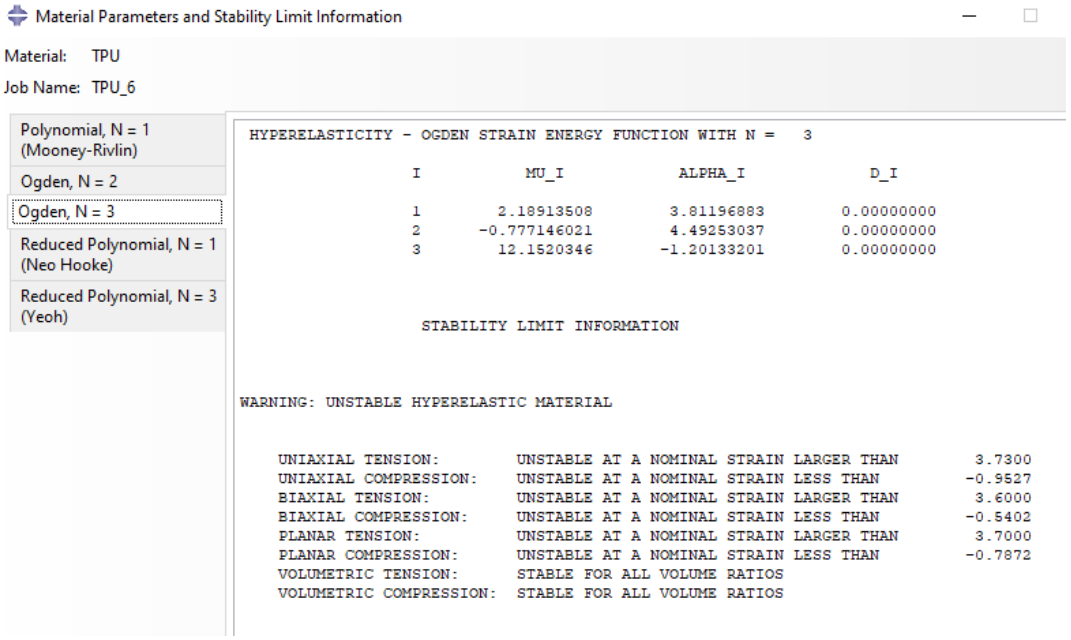

Figure 3.32 Material parameters and stability limit information returned by Abaqus of the Ogden N=3 Hyperelastic model.

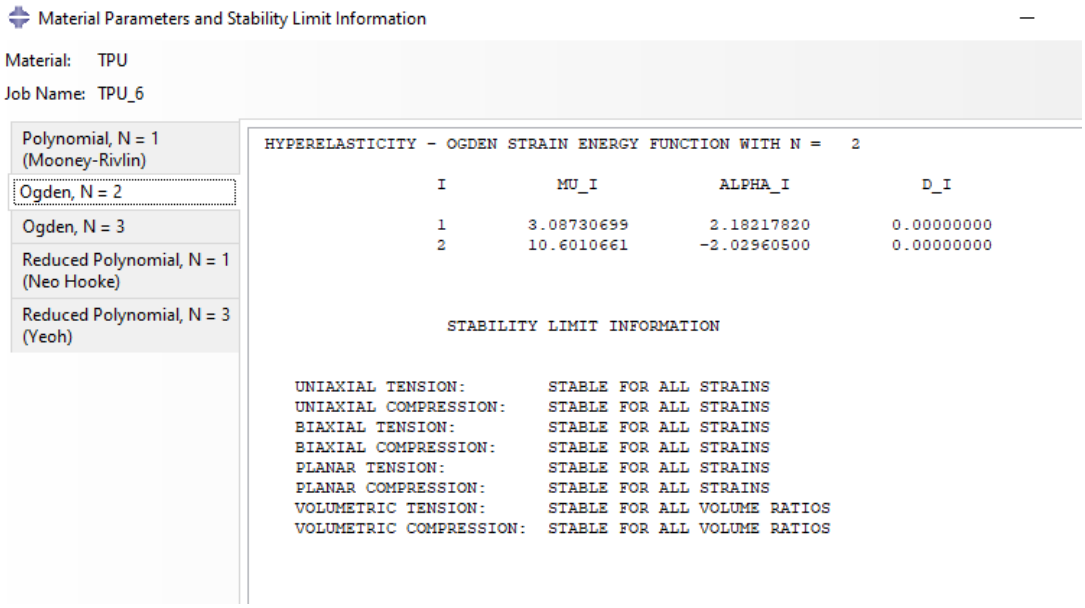

Figure 3.33 Material parameters and stability limit information returned by Abaqus of the Ogden N=2 Hyperelastic model.

As for the Ogden model of polynomial order 3, Abaqus reports instability condition (Figure 3.32), while in the Ogden model of polynomial order 2 the model is stable (Figure 3.33). Hence the choice of the hyperelastic model Ogden second order.

The geometry was imported from Onshape (Figure 3.34) and the mesh generation proceeded (Figure 3.34).

Since the geometry is complex, it was decided to use quadratic tetrahedes as elements, with hybrid formulation, condition imposed in case of hyperelastic material by the software (C3D10H).

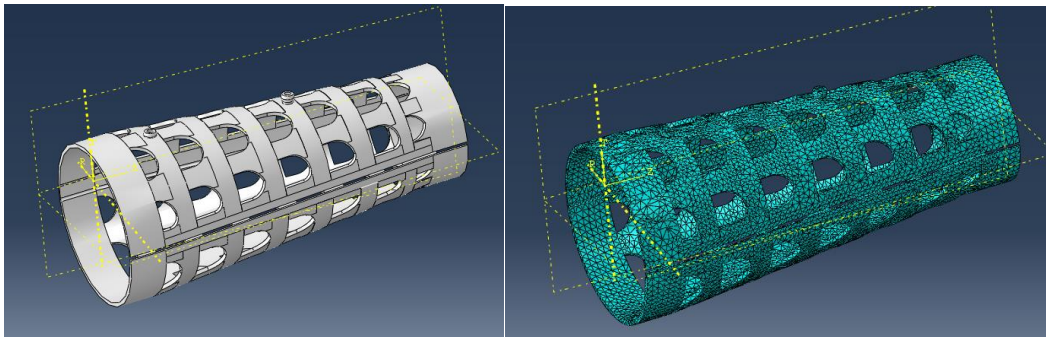

Figure 3.34 on the left it is shown the CAD geometry imported in Abaqus, on the right it is shown how the part has been meshed. It is also visible the reference system defined by planes solidar with the geometry

A convergence study was carried out for the choice of the number of elements and therefore the degree of refinement of the mesh. Simulations were conducted by constraining the vertical displacements and imposing a tangential displacement, in correspondence of the

device lateral slit, to simulate the opening of the device (Figure 3.35), by a cylindrical reference system created with the vertical axis integral with the inclination of the model.

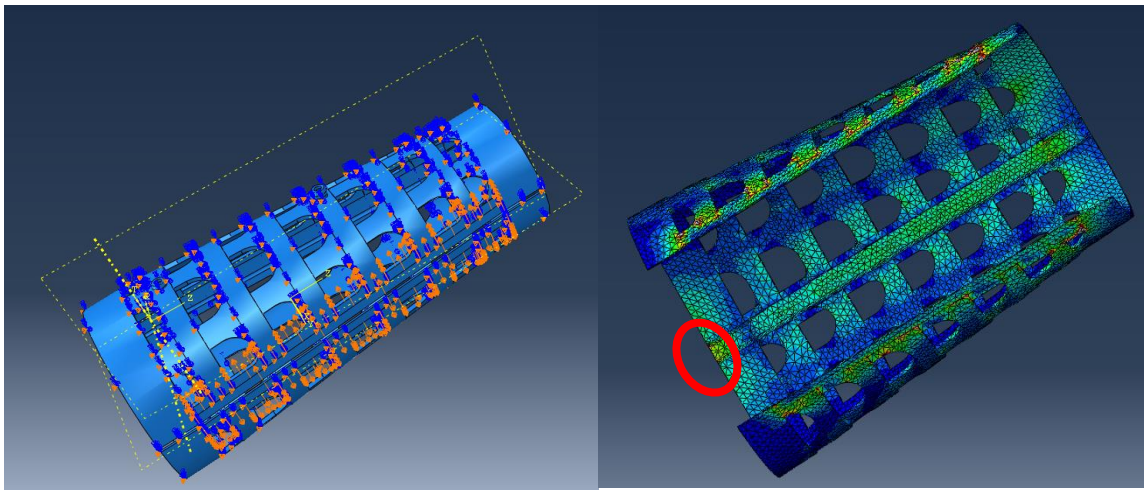

Figure 3.35 On the left image the boundary conditions are visible. The orange arrows represent the tangential displacement imposed and the blue one shows the constrains on the z axis. The right image shows the configuration after the job was ran. The structure has an open conformation and the most loaded point has been circled.

The most stressed area was evaluated (Figure 3.35), and the maximum stresses of Von Mises were then compared (it was averaged around the maximum stress area in order to compare different meshes). In figure 3.36 is shown the trend of the maximum Von Mises stresses as the mesh refinement increases.

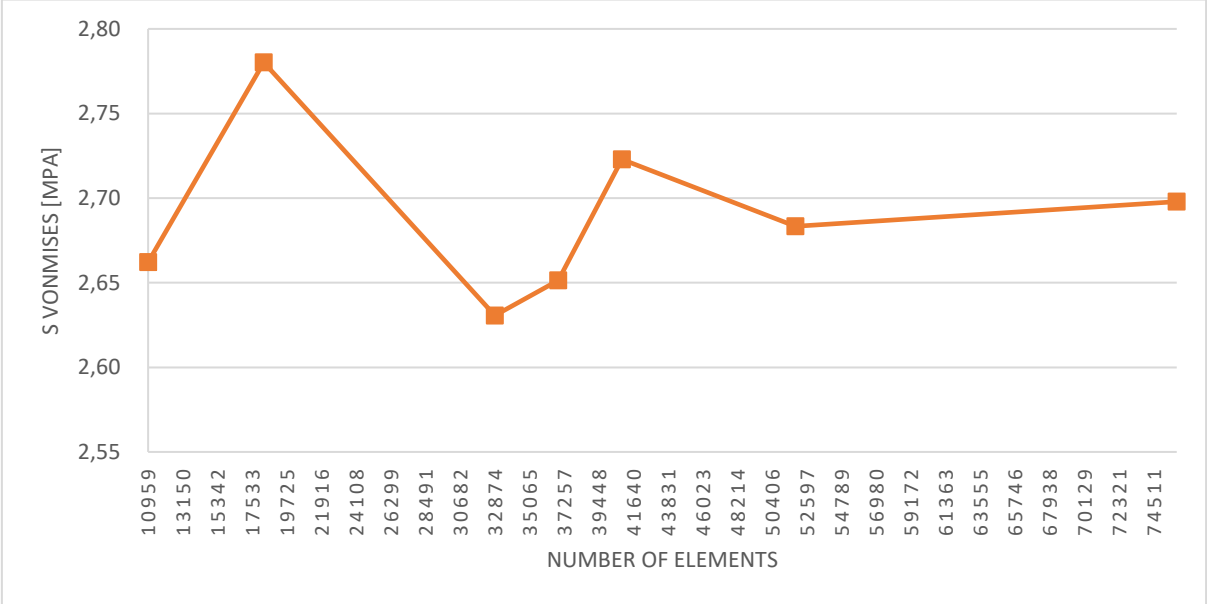

Figure 3.36 Convergence study. The horizontal axis shows the incremental number of faces while the vertical axis shows the resulting von Mises max stress corresponding to the mesh used in the most loaded area.

Convergence was considered reached when the difference between the value calculated by the current simulation and that calculated by the previous simulation was less than 2%. Convergence was achieved with a mesh of 41195 elements.
For the fatigue verification tree models were created with variable thickness, equal to 1,2 mm, 1 mm, 0,8 mm (Figure 3.37) in correspondence of the connection band, and constant thickness of 2 mm for the rest of the structure.

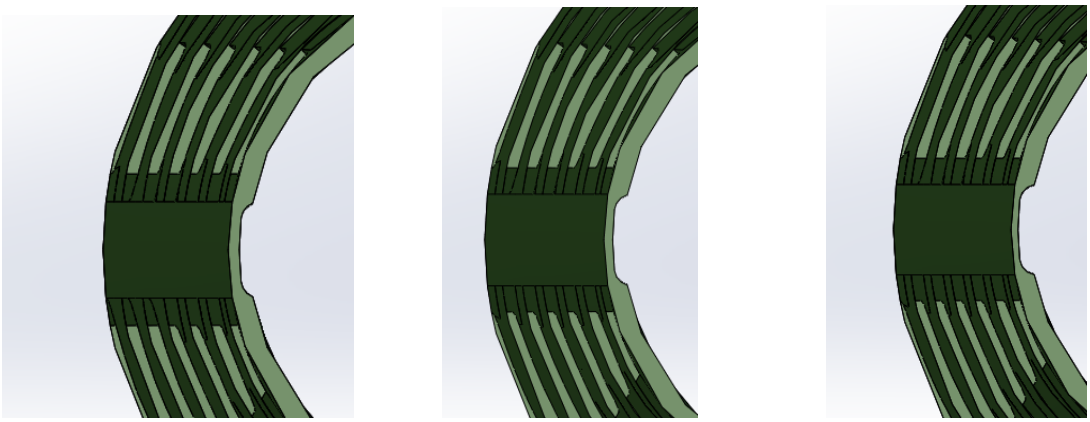

Figure 3.37 Comparison of variable thickness of the thin connection band. From the left is shown thickness of 1,2 mm, of 1 mm and of 0,8 mm.

Once the hyperelastic model was identified and the mesh chosen, the step (step type: static, general) was created, in which the boundary conditions was imposed: the vertical displacements were locked and was imposed a radial displacement with module of 40 mm in correspondence with the opening of the device.

Abaqus implicit was used as solver type (which uses the backward Euler algorithm) since it is an almost static problem and without interactions with other objects. Furthermore, the implicit solver allows to characterize the material as incompressible, which is the case in analysis.

3.3.3 Fit through reconstruction of the forearm

During the development phase of the various prototypes, the problem of fit was often encountered. It turned out to be complex to adapt rigid structures to anatomical segments, so these could be too wide or too thick and the result was the remaking of the print "by trial". This limit led to the decision to make a simulation of the wearability, reconstructing the

forearm in 3D and overlapping the electrode applicator. To verify that the model actually fits the user's measurements, it was decided to carry out a 3D reconstruction of a forearm, and then compare it with the electrode applicator model obtained by entering the measurements of the test candidate in Onshape, as illustrated in the chapter 3.2.1.5.
For the acquisition, the Scandy pro iOS application was used, which uses the iPhone's Trudepth camera technology to reconstruct three-dimensional images.

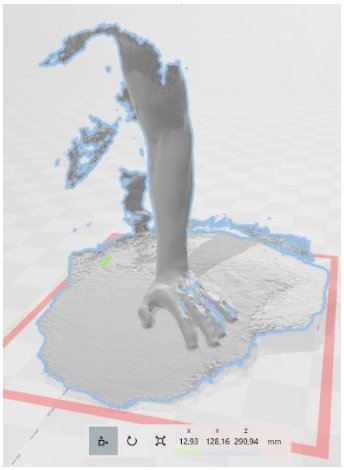

Figure 3.38 Computer imported scan. It appears how the cloud point is yet to be cleaned as the surroundings of the arm have been scanned aswell.

The scan, exported from the application in .STL format, appears as a point cloud (Figure 3.38). It was imported into the MeshLab opensource software where it was cleaned and repaired with special filters and a closed surface was created using the surface reconstruction screened Poisson tool. Was then smoothed with the Laplacian filter. The resulting surface is show in Figure 3.39.

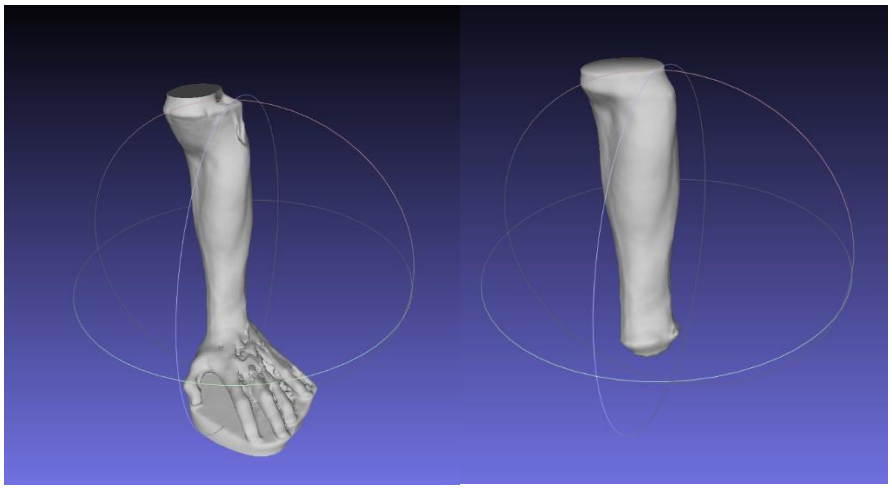

Figure 3.39 Point cloud imported and elaborated on Meshlab to obtain a surface mesh with the surface reconstruction screened Poisson tool.

The mesh obtained was imported in Autodesk Fusion 360 to scale it and adapt the number of meshes to our needs since CAD software such as Solidworks and Onshape cannot process meshes with number of faces > 5000. On Fusion 360, the number of meshes that identified the closed surface was therefore reduced, and the mesh was converted into a B-rep body type with the appropriate tool (Figure 3.40). The solid was then exported in .STEP format and opened on the Solidworks software, to be converted into .X_T format, ideal for import in Onshape. (this passage was necessary because the .X_T format is not an export option on Fusion 360)

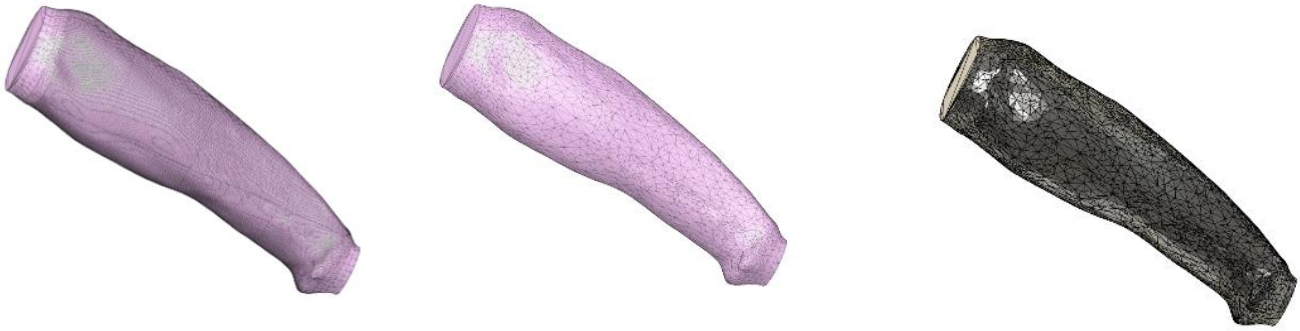

Figure 3.40 Mesh imported in Fusion360. From the left there is the surface mesh exported from MeshLab, the mesh reduction and the solid reconsructed with the tool “mesh in B-rep”.

The model was sectioned in Onshape near the proximal end of the ulna and at the wrist, creating the first surface in corrispondance with the radio styloid process (as an anatomical landmark) and offsetting the secon surface by the length of the forearm experimentally mesured (Figure 3.41). This is to create surfaces in correspondence with the positions in

which it is indicated to carry out the anatomical measurements to the user, as described in chapter 3.2.

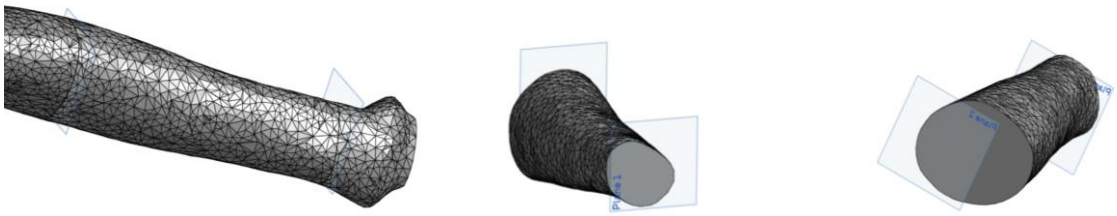

Figure 3.41 Distal forearm section, defined perpendicularly to the long axis of the arm in correspondence of the bone prominence of the wrist, and proximal section, offsetted from the distal section by the length of the forearm.

A verification was made of the correspondence between 3D reconstruction and experimental measurements of the forearm. The areas subtended by the spline that identifies the contour of the section were then compared with the areas subtended by the corresponding sketches in the drawing of the electrode applicator.

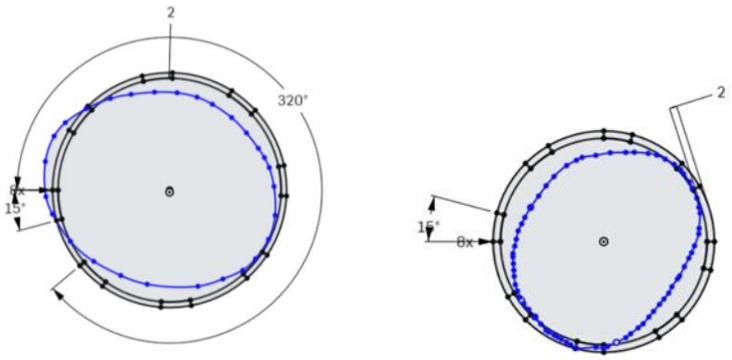

Figure 3.42 In blue is visible the spline that identify the contour of the forearm projected on the section previously created, in black the sketch of the prototype in its proximal (on the left) and distal (on the right) part.

The corresponding circumferences were then obtained as

$$D_{corrisponding} = 2\sqrt{\frac{Area_{spline}}{\pi}}$$

to have comparable parameters. The tests were carried out on 4 collaborators to verify measurement errors.

Chapter 4 RESULTS AND DISCUSSION

4.1 Abaqus Results

To verify the fatigue resistance of the cage connecting bar, the maximum deformation values obtained with the simulations were compared with the Wohler curve for TPU from the literature. The estimate of the use of the device assumes that it is opened twice a day (to put it on and to take it off), daily.

It is necessary to make some precautions:

As this is a do-it-yourself device, it is not possible to estimate parameters such as the size of the grains of the material (therefore the heat treatment undergone by the material), the presence of notches and the surface state, i.e. the surface roughness, since these depend on the printer and the printing techniques used. In fact, the choice of how to make it is up to the user.

It is also true that since it is an external orthosis, any breakage is not to be considered dangerous. Furthermore, being a hyperelastic material this does not undergo a fragile break. This verification therefore has the objective of verifying the appropriateness of the chosen material in this conformation, without this being a guarantee of duration.

In the results of the first test, i.e. with a thickness of the connection band of 1.2 mm, the point with the maximum strain values (Fig 4.1) was identified at the proximal end of the band. Since is a non linear geometry it has to be considered nonlinear strain component which in this case is logarithmic Strain (LE). With the Abaqus tool ‘query’, the strain values in the identified area were exported and plotted in Excel.

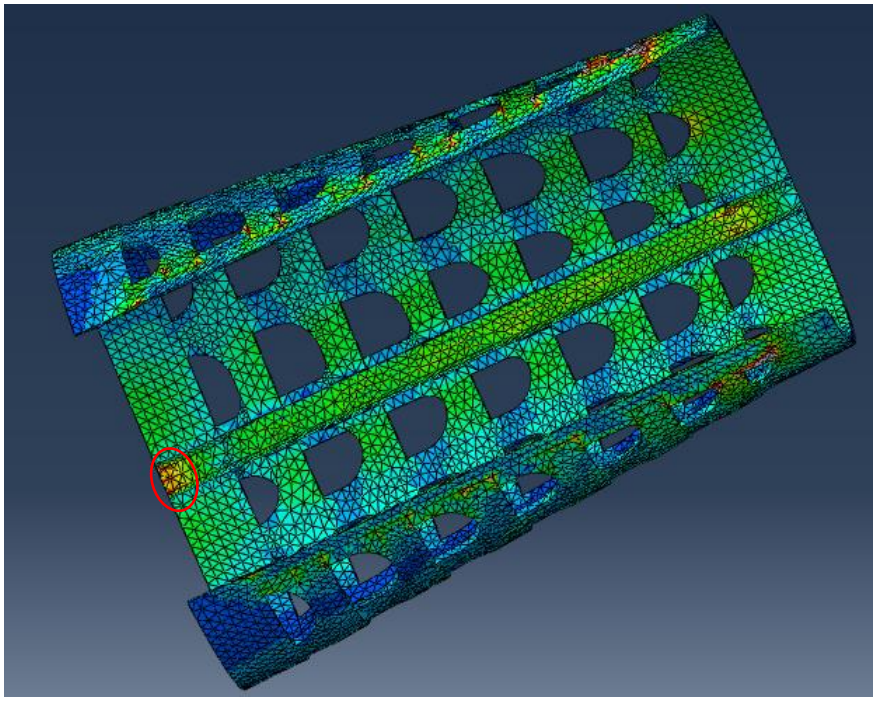

Figure 4.1 Simulation of the opening of the prototype by imposing a symmetrical tangent displacement of 40 mm. The area with maximal strains is circled in red.

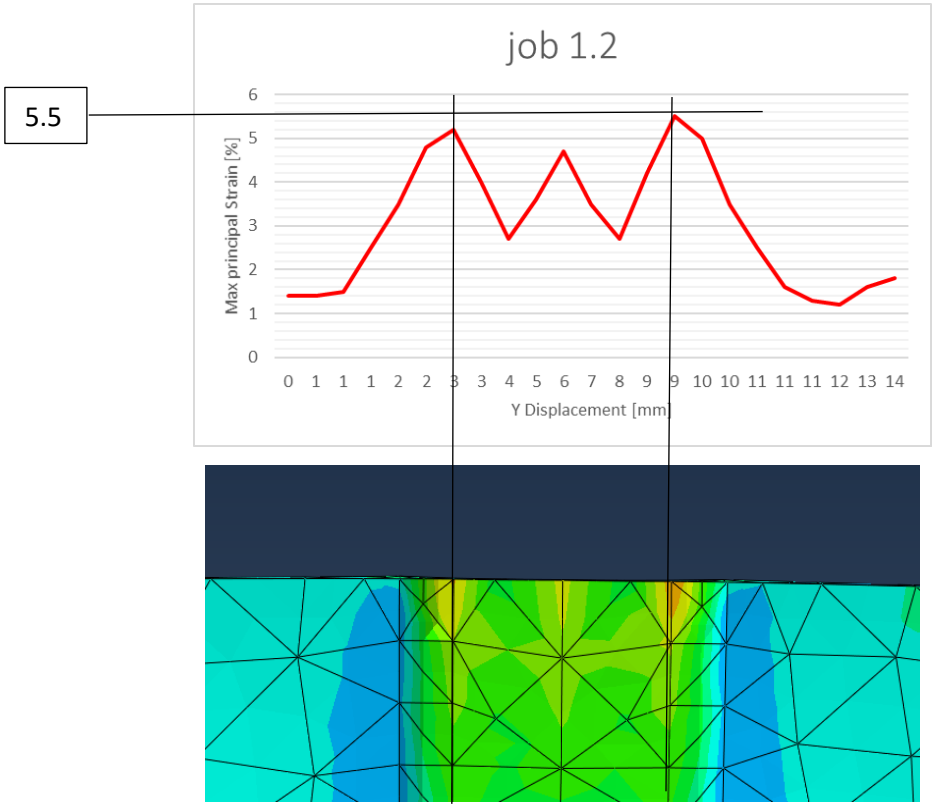

Figure 4.2 Deformation trend on the most loaded profile. The peak occurs at the junction between the 2 mm thick shell and the 1.2 mm thick thin band

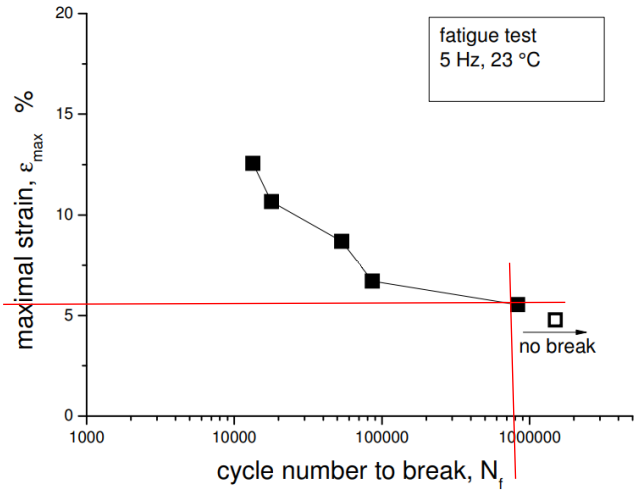

Figure 4.3 Graphical fatigue solution comparing the maximal strain obtained with the Wohler diagram of the material.

The results shows a maximum strain value of 5,5% (Figure 4.2) and compared with the Wohler diagram (Figure 4.3), from which a resistance <800000 cycles was referenced, in our case of use, this corresponds to life long duration.

The second test was done in the same way by varying the thickness of the thin band from 1.2 mm to 1 mm.

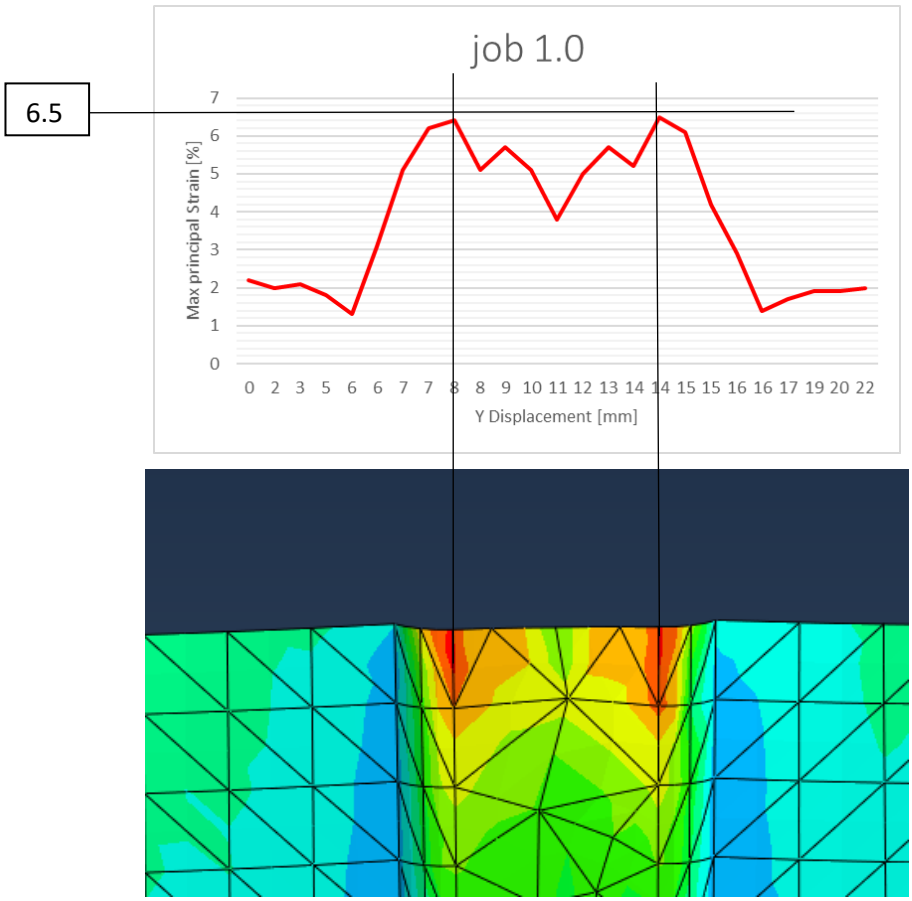

Figure 4.4 Deformation trend on the most loaded profile. The peak occurs at the junction between the 2 mm thick shell and the 1 mm thick thin band

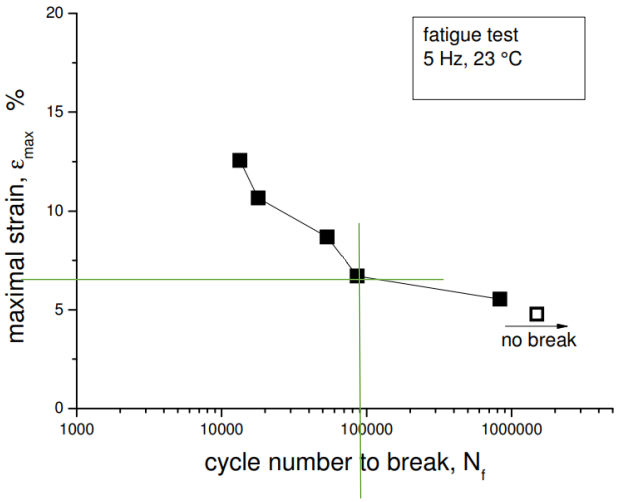

Figure 4.5 Graphical fatigue solution comparing the maximal strain obtained with the Wohler diagram of the material.

The results of the second test (Figure 4.4), ie with a thickness of the connection band of 1 mm, do not differ much from the previous case as a maximum deformation equal to 6,5% was evaluated. Similarly, the comparison with the Wholer diagram (Figure 4.5) gives a life long duration estimation.

The third test was done in the same way by varying the thickness of the thin band from 1 mm to 8 mm.

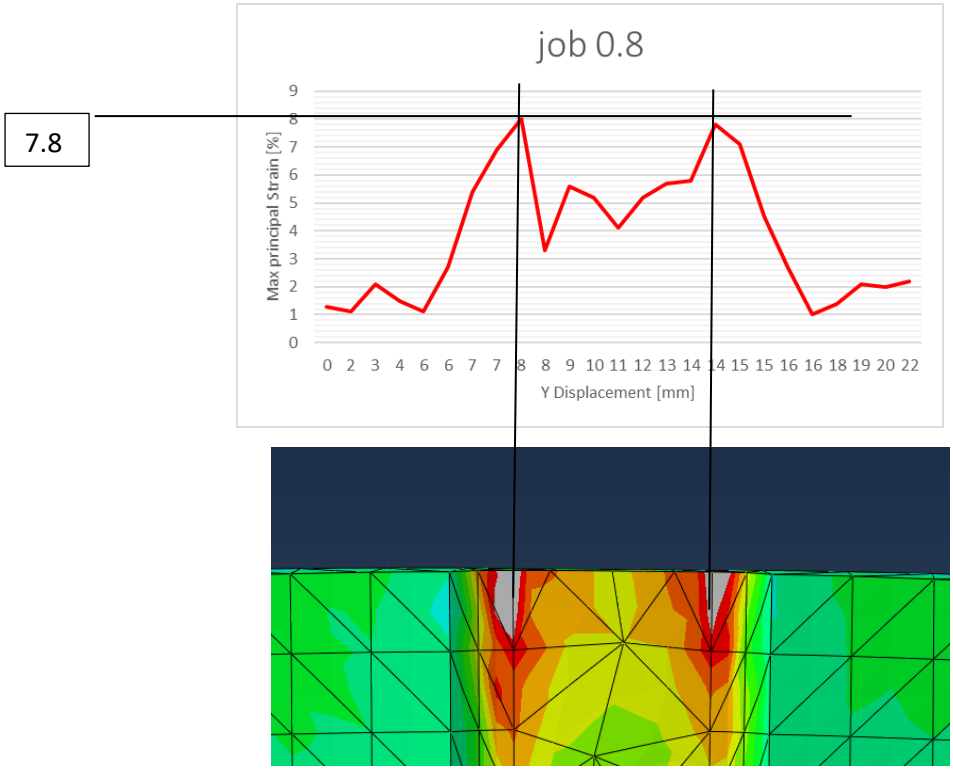

Figure 4.6 Deformation trend on the most loaded profile. The peak occurs at the junction between the 2 mm thick shell and the 8 mm thick thin band.

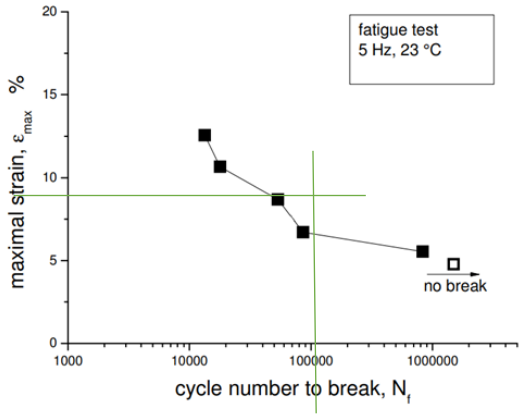

Figure 4.7 Graphical fatigue solution comparing the maximal strain obtained with the Wohler diagram of the material.

As regards the test with a thickness of 0.8 mm, the maximum strain evaluated is equal to 7,8% (Figure 4.6), which by comparison with the fatigue curve (Figure 4.7) implies a duration <70 years.

The analyzes carried out show an increase in strain as the section decreases. To clarify why, the stress strain variation data over the time of the test were extracted, calculated at the most loaded node which was verified to be node 548.

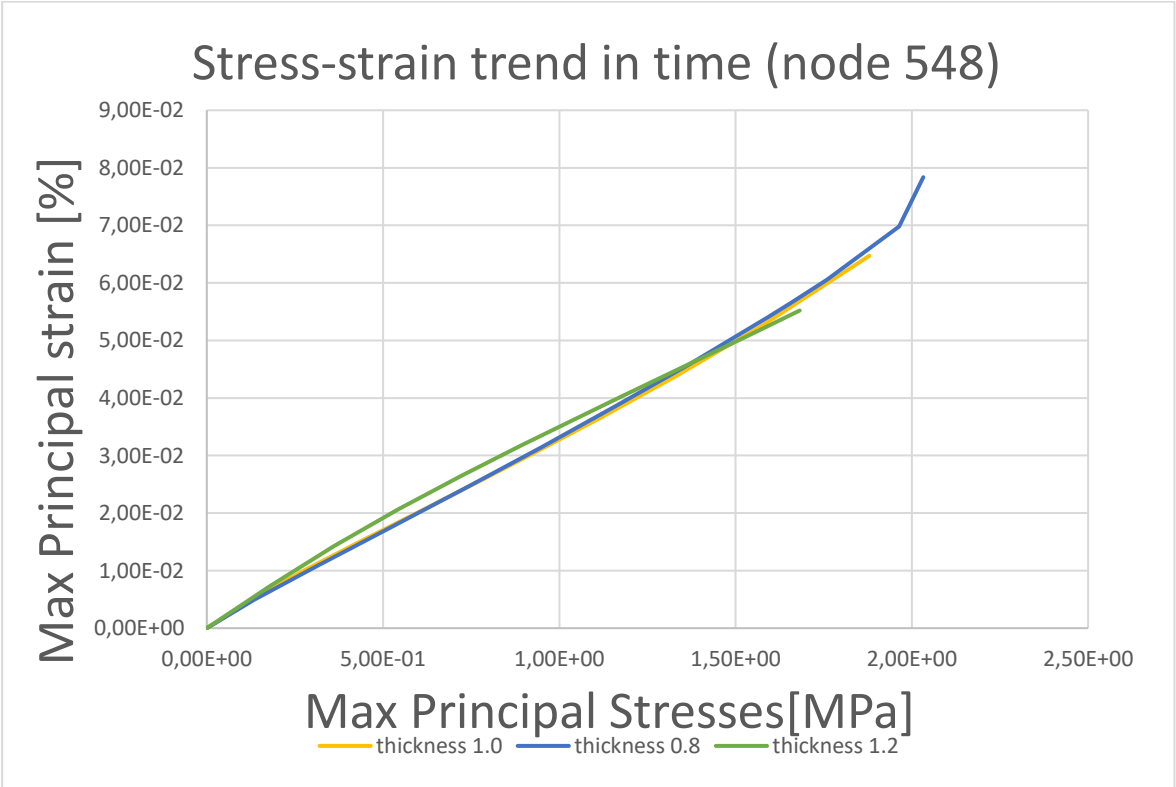

Figure 4.8 Plot of Max principal strain over Max principal stress in time in the most loaded node for thickness on 1.2 mm, 1 mm and 0.8 mm of the thin band.

At the beginning of the tests, as shown in Figure 4.8, the larger thickness model responds with greater deformations. However, it can be seen that the model with a smaller section achieves greater stress at the end of the test and consequently greater strains result. The reason for this was found in the fact that the initial displacement is applied to the 2 mm section shell. The most loaded point is the one where the model is beveled and there is the transition from a thickness of 2 mm to lesser thicknesses of the thin band. Therefore, the resulting increase in strain is due to the increase in stress derived from the discontinuity of the geometry.

In all cases analysed, the estimated life largely satisfies the needs, and this bodes well that the use of TPU is an acceptable choice in this type of application.

4.2 Fitting test

Due to the Covid-19 emergency it was not possible to arrange a meeting with a tetraplegic user, as had been done in the early planning stages. These tests were therefore performed on healthy collaborators and do not reflect the pathological conformation of an atrophic forearm. However, they give an idea of the inter variability of the model.

The space between the circumference that reflects the measurement of the forearm and that of the prototype drawing (i.e. the distance between the circumference of the measurement entered in the "antrodata" and the circumference that will actually be drawn by the program) is defined in the project as a variable " padding ”and takes into account the thickness of the electrodes that are placed between the applicator and the arm and gives an idea if the future print may fit too tight (uncomfortable to wear) or too loose (poor adhesion of the electrodes to the arm).By design this is defined as 2 mm.

The error considered is defined on the variation between the entered diameters and those obtained with the 3D reconstruction

$$e_{\%} = \frac{|D_s - D_r|}{D_r} \cdot 100$$

Where D_s is the simulated diameter and D_r is the real diameter, the one obtained by inserting the measurements obtained with the 3D reconstruction in the datasheet.

Since the electrode applicator will be molded in flexible material and the closure of the device will be made from velcro faces, which are also flexible and easy to hold, we can consider acceptable errors < 5%.

It should also be said that there is no unique protocol for measuring this anthropometric data. During the scanning from the forearm, the collaborators were asked to keep the arm as straight and still as possible, but it was not possible to use supports to fix its position because these would have affected the scanning itself. Consequently, the planes from which the measurements of the three-dimensional reconstructions are taken may be inclined with respect to the axis of the arm. The elbow crease and the wrist bones were kept as recognizable anatomical landmarks.

4.2.1 Test results on the first collaborator

The experimental measurements of the forearm of the first collaborator are:

PPdiam (proximal part diameter) = 97 mm

DPdiam (distal part diameter) = 64 mm

ArmLength (forearm length) =230 mm

From the 3D reconstruction (Figure 4.9), the areas subtended by the splines that identify the profile of the forearm on the section planes (Figure 4.10) appear to be respectively

$A_{PP} = 6501.93328\ mm^2$

$A_{DP} = 3129.983\ mm^2$

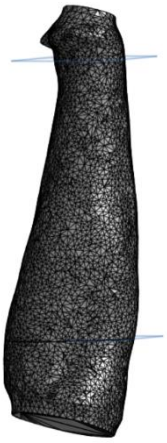

Figure 4.9 3D reconstruction of the first collaborator forearm.

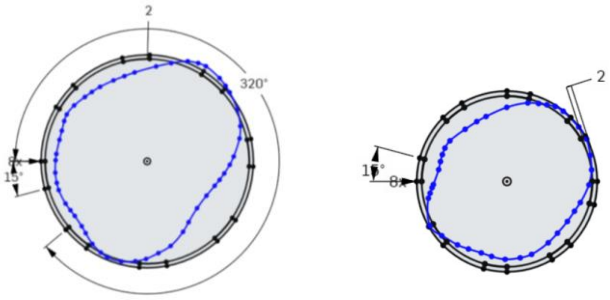

Figure 4.10 Overlap of the splines with the model sketches.

To this corresponds circumferences of diameter

$D_{PP} = 90{,}98\ mm$

$D_{DP} = 63{,}12\ mm$

In Figure 4.11 is the overlap between the CAD drawing sketch and the circumferences with corresponding diameter.

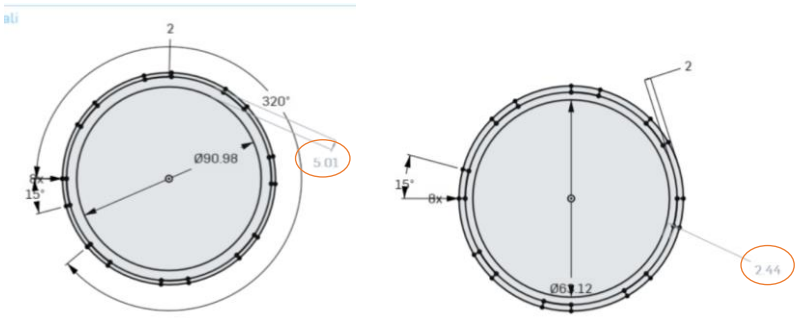

Figure 4.11 the internal circumference is the one obtained with the correspondent diameter. The distance with the model sketch is circled in red.

$e_{\%PP} = 6{,}61\%$ Padding = 5,01 mm

$e_{\%DP} = 1{,}39\%$ Padding = 2,44 mm

From these data it can be deduced that the model created through experimental measurements will be too loose in its proximal part.

This error may be due to the collaborator's highly developed musculature, which therefore makes it difficult to correctly position the caliber and make a direct accurate reading.

As mentioned at the beginning of the chapter, this condition should not occur in the case of tetraplegic users

4.2.2 Test results on the second collaborator

The experimental measurements of the forearm of the second collaborator are:

PPdiam = 77 mm

DPdiam = 52 mm

ArmLength =200 mm

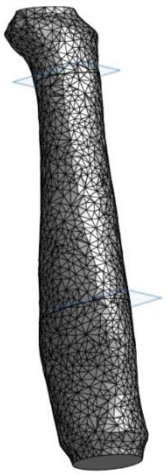

Figure 4.12 3D reconstruction of the second collaborator forearm.

From the 3D reconstruction (Figure 4.12), the areas subtended by the splines that identify the profile of the forearm on the section planes (Figure 4.13) appear to be respectively

$A_{PP} = 4685.768\ mm^2$

$A_{DP} = 2016.687\ mm^2$

To this corresponds circumferences of diameter

$D_{PP} = 77{,}24\ mm$

$D_{DP} = 50{,}76\ mm$

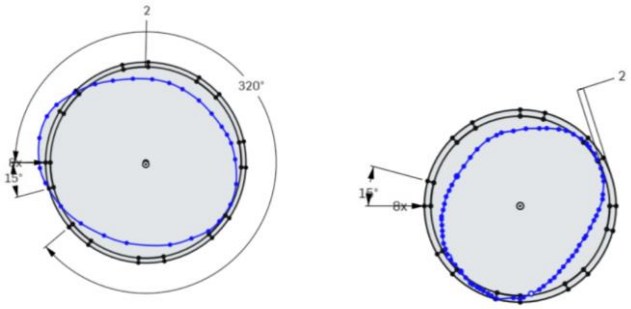

Figure 4.13 Overlap of the splines with the model sketches.

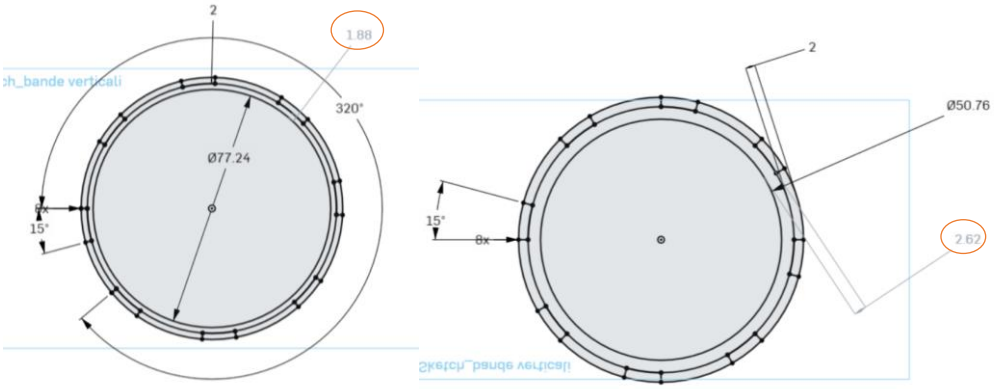

Figure 4.14 The internal circumference is the one obtained with the correspondent diameter. The distance with the model sketch is circled in red.

$e_{\%PP} = 0{,}3\%$ Padding=1,88 mm

$e_{\%DP} = 2{,}44\%$ Padding = 2,62 mm

The second collaborator has a thinner arm coformation, this is reflected in the errors that are negligible. In this case, the device should adhere properly to the arm.

4.2.3 Test results on the third collaborator

The experimental measurements of the forearm of the third collaborator are:

PPdiam = 89 mm

DPdiam = 59 mm

ArmLength =225 mm

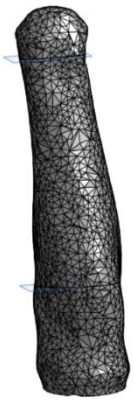

Figure 4.15 3D reconstruction of the third collaborator forearm.

From the 3D reconstruction (Figure 4.15), the areas subtended by the splines that identify the profile of the forearm on the section planes appear to be respectively

$A_{PP} = 6587{,}348\ mm^2$

$A_{DP} = 2577{,}847\ mm^2$

To this corresponds circumferences of diameter

$D_{PP} = 91{,}58\ mm$

$D_{DP} = 57{,}29\ mm$

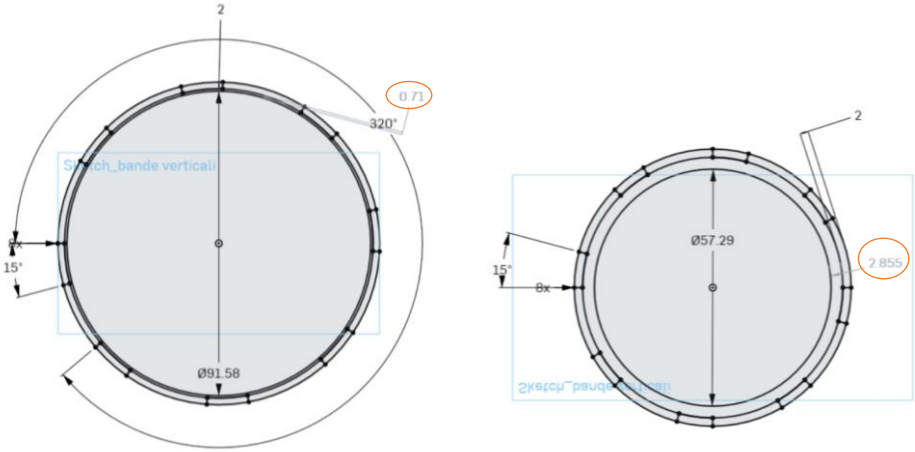

Figure 4.16 The internal circumference is the one obtained with the correspondent diameter. The distance with the model sketch is circled in red.

$e_{\%PP} = 2{,}81\%$ Padding=0,71 mm

$e_{\%DP} = 2{,}98\%$ Padding = 2,85 mm

The third collaborator has a sturdy but slender structure. Also in this case the errors found do not exceed the proposed threshold.

4.2.4 Test results on the fourth collaborator

The experimental measurements of the forearm of the fourth collaborator are:

PPdiam = 80 mm

DPdiam = 53 mm

ArmLength =210 mm

Figure 4.17 reconstruction of the fourth collaborator forearm.

From the 3D reconstruction, the areas subtended by the splines that identify the profile of the forearm on the section planes appear to be respectively

$A_{PP} = 6587{,}348\ mm^2$

$A_{DP} = 2577{,}847\ mm^2$

To this corresponds circumferences of diameter

$D_{PP} = 78{,}775\ mm$

$D_{DP} = 55{,}953\ mm$

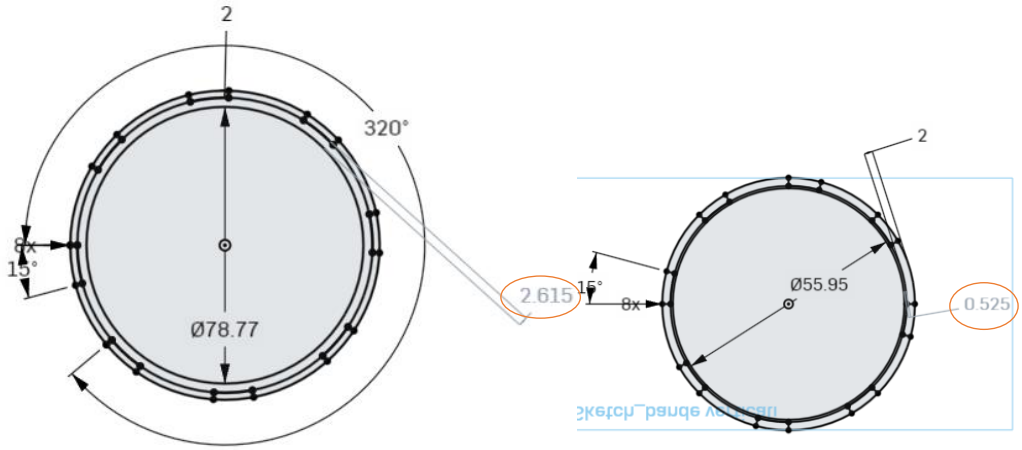

Figure 4.18 The internal circumference is the one obtained with the correspondent diameter. The distance with the model sketch is circled in red.

$e_{\%PP} = 1{,}56\%$ Padding=2,61 mm

$e_{\%DP} = 5{,}27\%$ Padding = 0,525 mm

In this last case the test concludes that the model would be to tight in its distal part.

To verify the error for this candidate, it was made the choice of printing a prototipe from the experimental mesurements. The results are show in the next chapter

4.3 Final prototype features

The printing of the final prototype was commissioned to stampaMI 3D, who made the piece in 24 hours at a cost of 20 euros. It was made of TPU 95A with the following printing characteristics:

Layer height : 0,2 mm

Extrusion temperature : 230C
Bed temperature : 60c
Extrusion speed : 30 mm/sec

The piece results flexible at the thin band as desired. The side holes allow the passage of the wiring from the electrodes to the MeCFES control unit, and ensure the structure is extremely light. The TPU is comfortable in contact with the skin. Figure 4.19 shows the appearance of the assembly of the electrode applicator with the boxes for the electronic components worn on the arm of the candidate. The first verification carried out was to evaluate how the errors foreseen by the fitting tests affected the fit. Despite the under sizing, the flexibility of the material and the Velcro straps allow you to easily adapt the model to the shape of the arm. This indicates that the proposed margin of error is too restrictive and that direct measurements of the anthropometric data are sufficient to produce a structure that is sufficiently compliant to their needs.
Due to the Covid-19 emergency it was not possible to find a working MeCFES, so an old prototype was used to test the assembly.
By following the steps described in chapter 3.2.1.5 it was possible to build the device using components found at home. The Velcro was cut from an old cosmetic bag and fixed with a stapler, and a prototype box for the electronics was successfully fixed with buttons. The points of application of the electrodes had previously been evaluated for the subject, then an attempt was made to reproduce their positioning against photographs.
Wearing is simple and fluid thanks to the cylindrical preformed print that allows the positioning of the forearm in a guided manner, with the foresight to be performed on the edge of a table so that the closure can be wrapped sideways without the need for aid or arm twisting.
Once worn, the device is comfortable, but does not allow the complete twisting of the arm.
In the following chapter is given a specific cost estimation.

Figure 4.19 from the top left is show the assembly of the device with the MeCFES prototype, the open configuration with the placement of the electrodes subject specific, the wearing phases and the twisting of the forearm.

Net of the tests carried out, it is possible to summarize the characteristics of the final prototype in the following table:

Requirements	Final Prototype
Optimal fit	Ok The cage is adaptable to the user's measurements as shown in the fitting test. The grid allows you to freely position the electrodes ensuring the achievement of the optimal position for stimulation.
Support the physiological movements of the forearm	So and so The TPU grid allows some movement and thanks to the Velcro closure ensures excellent adherence between electrodes and skin during physiological movements.
Comfortable	Ok Having only used flexible materials it feels comfortable
Easily worn independently by the user	Ok With the use of therapeutic Velcro it resemble traditional orthotic closures to which users are accustomed
Do-it-yourself	Ok As described in the chapter 3.2.1.5, the construction steps are easily understood and achievable
Low cost	Ok The material used and the production technique allow to make the device affordably

Table 4.1 Project requirement for the second prototype

4.4 Estimation of construction costs

As reported in the literature, there are currently no devices on the market that have the same characteristics as MeCFES for home use. However, an estimate of the costs of making our DIY device will be proposed and these will be compared with the Omnihi5™ (electrostimulator with the possibility of myoelectric control, not yet approved by the FDA or the EMA but on sale in Australia) and with the H200 (electrostimulator with manual control on the market).

Several online quotes were requested for the 3D printing of the components of the final prototype. There is a wide price variability with regard to the TPU piece. Given the conformation of the piece, the choice of the quantity of use of the PVA support is up to the producers, as well as that of the printing speed, based on the printers that each of them has.

Estimates range from 400 euros (abprint3d) to 150 euros (vectorealism) to 95 euros (stampa3dservizi), while for the PLA boxes the price is fairly consistent and is around 15 euros per component.

Another possibility is to rely on non-professional makers. Browsing on pages such as subito.it, Facebook and Instagram, many hobbyists have been discovered who, owning personal printers, offer the printing service at even cheaper prices.

An example of this is GR3D and StampaMI 3D, which have proposed corresponding quotes of 50 and 20 euros for the TPU piece and 10 and 5 euros for the PLA components (price per piece).

For the other components required for assembly, the following prices have been estimated:

BlackBerry Curve 8520: between 15 euros (eBay price) and 30 euros (Facebook marketplace price)

Flexible Velcro bandages: 3 euros per meter (haberdashery)

Snap buttons: set of 100 pieces for 8 euros on amazon, a few cents per piece in haberdashery.

Plastic rings: 10 pieces for 3 euros on amazon, a few cents per piece in haberdashery

Electronic card: 100 euros

EMG electrodes with button connection: 100 pieces for 12 euro on amazon (it is recommended the purchase of many pieces as they will be periodically replaced)

Stimulation electrodes with plug connection: 48 pieces for 20 euros.

Synthetic deerskin cloth: 10-15 euros (amazon, supermarket)

The estimate was based on the geographical area of Milan and province and may vary if purchases are made from other regions.

For the printable components was taken into account the minimum price estimated through online services, which allow shipments throughout Italy, with the consideration that through a more in-depth research by the user this price can further reduce.

The total estimated price, which considers the frequent replacement of the electrodes, is about 300 euros, in addition to the time of realization.

As for commercially available products, the information found online assigns a cost between $ 3,000 and $ 5,000 for the H200 and $ 3,500 for the OmniHi5™.

Chapter 5 CONCLUSIONS

In this thesis, the goal was to create a MeCFES applicator device that was patient-specific and self-built by the consumer. This had to be comfortable, easy to wear, support the anatomical movements of the forearm and economical. Another objective was to make the design participatory, involving the users to whom it is addressed to make it conform to their needs, thus avoiding the common problem of abandonment in use. To do this, a process of development of several prototypes was followed, to be created with 3D printing. 3D printers are very versatile tools, both in development and in production. Thanks to these it was possible to quickly shape ideas and make immediate practical assessments, discarding or promoting solutions based on the direct use of prototypes. It has been verified how these allow the creation of tailor-made models, without having to define standard sizes.

The use of Onshape for the design has allowed the creation of a parametric model, and therefore editable in first person by the user. This involves the elimination of intermediate

figures between the user and the manufacturer. In fact, it is not necessary to rely on professionals to make the model tailored, but it has been shown that it is enough to enter 3 easily measurable parameters to obtain a product that meets the required needs.
Thanks to computational tests, it has been demonstrated how the chosen material amply bears the conditions of use and how it allows a correct assembly of all components. The Co-design experience has shown how user involvement can inspire more effective solutions and meet specific needs.
From the estimate costs of construction, it can be said that this device is much cheaper than the prices of commercial products, and therefore it is affordable for a much wider audience. The hope is that its contained pricing will entice more and more users to invest their time to build it, thus making this technology within everyone's reach.
Please note that the device was designed to be a DIY product, not a commercial product. It is therefore devoid of official guarantees and certifications.

5.1 Limitations and future developments

The major limitation of this project lies in not having carried out a functionality check of the final product on a tetraplegic user. This would be a starting point for opening a systematic study involving a much larger number of participants in order to collect data and feedback. It will be necessary to investigate the use of even more flexible materials to further favor anatomical movements but which at the same time can withstand the support of MeCFES and its components and allow for correct application.
An ideal future development would be to involve rehabilitation centers in the project. These could propose MeCFES and its applicator directly to the tetraplegic user as AD, providing technical support for the specific patient adaptation, calibration, and assembly phase.

Chapter 6 BIBLIOGRAPHY

[1] S. L. Garber and T. L. Gregorio, “Upper extremity assistive devices: assessment of use by spinal cord-injured patients with quadriplegia.,” *The American journal of occupational therapy. : official publication of the American Occupational Therapy Association*, vol. 44, no. 2. American Occupational Therapy Association, pp. 126–131, Feb. 01, 1990, doi: 10.5014/ajot.44.2.126.

[2] P. J. Manns and K. E. Chad, “Components of quality of life for persons with a quadriplegic and paraplegic spinal cord injury,” *Qual. Health Res.*, vol. 11, no. 6, pp. 795–811, Nov. 2001, doi: 10.1177/104973201129119541.

[3] “Position of function hand.” https://somepomed.org/articulos/contents/mobipreview.htm?9/61/10197 (accessed Nov. 22, 2020).

[4] “Terapia Occupazionale: Ortesi statiche per l’arto superiore.” https://www.simonefiscarelli.com/2017/10/terapia-occupazionale-ortesi-statiche.html (accessed Nov. 09, 2020).

[5] “RO+TEN s.r.l.” https://it.orthoservice.com/ (accessed Nov. 22, 2020).

[6] “Order the SaeboGlove Hand Therapy Glove for Stroke Patients.” https://www.saebo.com/shop/saeboglove/ (accessed Nov. 09, 2020).

[7] E. Biddiss and T. Chau, “Upper-Limb Prosthetics,” *Am. J. Phys. Med. Rehabil.*, vol. 86, no. 12, pp. 977–987, Dec. 2007, doi: 10.1097/PHM.0b013e3181587f6c.

[8] K. A. Raichle *et al.*, “Prosthesis use in persons with lower- and upper-limb amputation,” *J. Rehabil. Res. Dev.*, vol. 45, no. 7, pp. 961–972, 2008, doi: 10.1682/JRRD.2007.09.0151.

[9] “NOMENCLATORE TARIFFARIO DELLE PROTESI ELENCO N. 1 : Nomenclatore tariffario delle prestazioni sanitarie protesiche.”

[10] D. B. Popović, “Advances in functional electrical stimulation (FES),” *Journal of Electromyography and Kinesiology*, vol. 24, no. 6. Elsevier Ltd, pp. 795–802, Dec. 01,

2014, doi: 10.1016/j.jelekin.2014.09.008.

[11] C. Bustamante, F. Brevis, S. Canales, S. Millón, and R. Pascual, “Effect of functional electrical stimulation on the proprioception, motor function of the paretic upper limb, and patient quality of life: A case report,” *J. Hand Ther.*, vol. 29, no. 4, pp. 507–514, Oct. 2016, doi: 10.1016/j.jht.2016.06.012.

[12] J. Jonsdottir *et al.*, “Arm rehabilitation in post stroke subjects: A randomized controlled trial on the efficacy of myoelectrically driven FES applied in a task-oriented approach.,” *PLoS One*, vol. 12, no. 12, p. e0188642, Dec. 2017, doi: 10.1371/journal.pone.0188642.

[13] R. Thorsen and M. Ferrarin, “Battery powered neuromuscular stimulator circuit for use during simultaneous recording of myoelectric signals,” *Med. Eng. Phys.*, vol. 31, no. 8, pp. 1032–1037, 2009, doi: 10.1016/j.medengphy.2009.06.006.

[14] P. Sampson *et al.*, “Using Functional Electrical Stimulation Mediated by Iterative Learning Control and Robotics to Improve Arm Movement for People with Multiple Sclerosis,” *IEEE Trans. Neural Syst. Rehabil. Eng.*, vol. 24, no. 2, pp. 235–248, 2016, doi: 10.1109/TNSRE.2015.2413906.

[15] S. Mangold, T. Keller, A. Curt, and V. Dietz, “Transcutaneous functional electrical stimulation for grasping in subjects with cervical spinal cord injury,” *Spinal Cord*, vol. 43, no. 1, pp. 1–13, Jan. 2005, doi: 10.1038/sj.sc.3101644.

[16] F. Inanici, S. Samejima, P. Gad, V. R. Edgerton, C. P. Hofstetter, and C. T. Moritz, “Transcutaneous electrical spinal stimulation promotes long-term recovery of upper extremity function in chronic tetraplegia,” *IEEE Trans. Neural Syst. Rehabil. Eng.*, vol. 26, no. 6, pp. 1272–1278, Jun. 2018, doi: 10.1109/TNSRE.2018.2834339.

[18] M. Shapiro, U. Gottlieb, and S. Springer, “Optimizing neuromuscular electrical stimulation for hand opening,” *Somatosens. Mot. Res.*, vol. 36, no. 1, pp. 63–68, Jan. 2019, doi: 10.1080/08990220.2019.1587401.

[19] P. H. Peckham, E. B. Marsolais, and J. T. Mortimer, “Restoration of key grip and release in the C6 tetraplegic patient through functional electrical stimulation,” *J. Hand Surg. Am.*, vol. 5, no. 5, pp. 462–469, Sep. 1980, doi: 10.1016/S0363-5023(80)80076-1.

[20] R. Thorsen, M. Ferrarin, R. Spadone, and C. Frigo, “Functional Control of the Hand in Tetraplegics Based on Residual Synergistic EMG Activity,” *Artif. Organs*, vol. 23, no. 5, pp. 470–473, May 1999, doi: 10.1046/j.1525-1594.1999.06362.x.

[21] R. A. Thorsen, E. Occhi, S. Boccardi, and M. Ferrarin, “Functional electrical stimulation reinforced tenodesis effect controlled by myoelectric activity from wrist extensors,” vol. 43, no. 2, pp. 247–256, doi: 10.1682/JRRD.2005.04.0068.

[22] R. Thorsen, R. Spadone, and M. Ferrarin, “A pilot study of myoelectrically controlled FES of upper extremity,” *IEEE Trans. Neural Syst. Rehabil. Eng.*, vol. 9, no. 2, pp. 161–168, 2001, doi: 10.1109/7333.928576.

[23] “OmniHi5™ Advanced FES Upper Extremity Treatment System Evidence Supporting FES 1,” 2019.

[24] M. Controlled and F. Electrical, “Rune Thorsen,” 2005.

[25] rthorsen, “Thorsen Thesis Appendix A. Marketing Analysis,” pp. 1–17.

[26] R. Thorsen and A. Medico, “Technology Management. Development of a Myo-electrical Controlled Functional Electrical Stimulator (MeCFES). (Business report, Erhvervsrapport),” no. February 1997, pp. 1–22, 1997.

[27] L. de Couvreur and R. Goossens, “Design for (every)one: Co-creation as a bridge between universal design and rehabilitation engineering,” *CoDesign*, vol. 7, no. 2, pp. 107–121, Jun. 2011, doi: 10.1080/15710882.2011.609890.

[28] R. Thorsen, F. Bortot, and A. Caracciolo, “From patient to maker - a case study of co-designing an assistive device using 3D printing,” *Assist. Technol.*, pp. 1–7, Jul. 2019, doi: 10.1080/10400435.2019.1634660.

[29] E. B.-N. Sanders and P. J. Stappers, “Co-creation and the new landscapes of design,” *CoDesign*, vol. 4, no. 1, pp. 5–18, Mar. 2008, doi: 10.1080/15710880701875068.

[30] J. Wherton, P. Sugarhood, R. Procter, S. Hinder, and T. Greenhalgh, “Co-production in practice: How people with assisted living needs can help design and evolve technologies and services,” *Implement. Sci.*, vol. 10, no. 1, p. 75, May 2015, doi: 10.1186/s13012-015-0271-8.

[31] W. Ben Mortenson, A. Pysklywec, M. J. Fuhrer, J. W. Jutai, M. Plante, and L. Demers, “Caregivers’ experiences with the selection and use of assistive technology,” *Disabil. Rehabil. Assist. Technol.*, vol. 13, no. 6, pp. 562–567, Aug. 2018, doi: 10.1080/17483107.2017.1353652.

[32] P. Johnston, L. M. Currie, D. Drynan, T. Stainton, and L. Jongbloed, “Getting it ‘right’: How collaborative relationships between people with disabilities and professionals can lead

to the acquisition of needed assistive technology," *Disabil. Rehabil. Assist. Technol.*, vol. 9, no. 5, pp. 421–431, Sep. 2014, doi: 10.3109/17483107.2014.900574.

[33] A. A. Portnova, G. Mukherjee, K. M. Peters, A. Yamane, and K. M. Steele, "Design of a 3D-printed, open-source wrist-driven orthosis for individuals with spinal cord injury," *PLoS One*, vol. 13, no. 2, Feb. 2018, doi: 10.1371/journal.pone.0193106.

[34] A. Manero *et al.*, "Implementation of 3D printing technology in the field of prosthetics: Past, present, and future," *Int. J. Environ. Res. Public Health*, vol. 16, no. 9, May 2019, doi: 10.3390/ijerph16091641.

[35] "Enabling The Future – A Global Network Of Passionate Volunteers Using 3D Printing To Give The World A 'Helping Hand.'" http://enablingthefuture.org/ (accessed Nov. 22, 2020).

[36] "Olivetti 3D S2 | Olivetti SPA." https://www.olivetti.com/it/archivio/olivetti-3d-s2 (accessed Nov. 22, 2020).

[37] "Ultimaker S5: affidabilità su larga scala." https://ultimaker.com/it/3d-printers/ultimaker-s5 (accessed Nov. 22, 2020).

[38] "Bobina Maxi - PLA bianco Sharebot: filamento PLA per stampa 3D 2,2 kg 1,75mm | Sharebot Monza." https://www.3dstoremonza.it/prodotto/filamento-pla-bianco-sharebot-bobina-maxi/ (accessed Nov. 22, 2020).

[39] "Filamento per stampante 3D RS PRO, PLA, Nero, diam. 1.75mm | RS Components." https://it.rs-online.com/web/p/materiali-di-stampa-3d/8320406/ (accessed Nov. 09, 2020).

[40] B. Wittbrodt and J. M. Pearce, "The effects of PLA color on material properties of 3-D printed components," *Addit. Manuf.*, vol. 8, pp. 110–116, Oct. 2015, doi: 10.1016/j.addma.2015.09.006.

[41] "Filamento per stampante 3D RS PRO, PVA, diam. 2.85mm | RS Components." https://it.rs-online.com/web/p/materiali-di-stampa-3d/8320494/ (accessed Nov. 09, 2020).

[42] "F000083 | Filamento per stampante 3D BQ, Filaflex, Bianco, diam. 1.75mm | RS Components." https://it.rs-online.com/web/p/materiali-di-stampa-3d/1362740/ (accessed Nov. 09, 2020).

[43] M. Shahzad, A. Kamran, M. Z. Siddiqui, and M. Farhan, "Mechanical characterization and FE modelling of a hyperelastic material," *Mater. Res.*, vol. 18, no. 5, pp. 918–924, Sep. 2015, doi: 10.1590/1516-1439.320414.

[44] Z. Major, M. C. Miron, and U. D. Cakmak, “Characterization of thermoplastic elastomers for design efforts,” in *Advanced Materials Research*, 2014, vol. 905, pp. 161–166, doi: 10.4028/www.scientific.net/AMR.905.161.

[45] W. MARS and A. FATEMI, “A literature survey on fatigue analysis approaches for rubber,” *Int. J. Fatigue*, vol. 24, no. 9, pp. 949–961, Accessed: Nov. 25, 2020. [Online]. Available: https://www.academia.edu/2969202/A_literature_survey_on_fatigue_analysis_approaches_for_rubber.

[46] A. Breitbarth, T. Schardt, C. Kind, J. Brinkmann, P.-G. Dittrich, and G. Notni, “Measurement accuracy and dependence on external influences of the iPhone X TrueDepth sensor,” in *Photonics and Education in Measurement Science 2019*, Sep. 2019, vol. 2019, no. 17, p. 7, doi: 10.1117/12.2530544.

[47] J. Alfaro-Santafé, A. Gómez-Bernal, C. Lanuza-Cerzócimo, J. V. Alfaro-Santafé, A. Pérez-Morcillo, and A. J. Almenar-Arasanz, “Three-axis measurements with a novel system for 3D plantar foot scanning: iPhone X,” *Footwear Sci.*, vol. 12, no. 2, pp. 123–131, May 2020, doi: 10.1080/19424280.2020.1734867.

[48] “Guida al Bridge perfetto - Ponti e sbalzi con stampante 3D FDM.” https://www.stampa3d-forum.it/guida-al-bridge-perfetto-ponti-e-sbalzi-con-stampante-3d-fdm/ (accessed Dec. 01, 2020).

[49] “Polsino con velcro e anello in plastica – NL Neolab sa.” https://www.neolab.ch/prodotto/polsino-con-velcro-e-anello-in-plastica/ (accessed Nov. 22, 2020).

[50] “Abaqus/CAE User’s Manual Abaqus 6.11 Abaqus/CAE User’s Manual.”

APPENDIX A

In the first sketch the profile of the prototype was drawn in a parametric way (Figure 6.1).

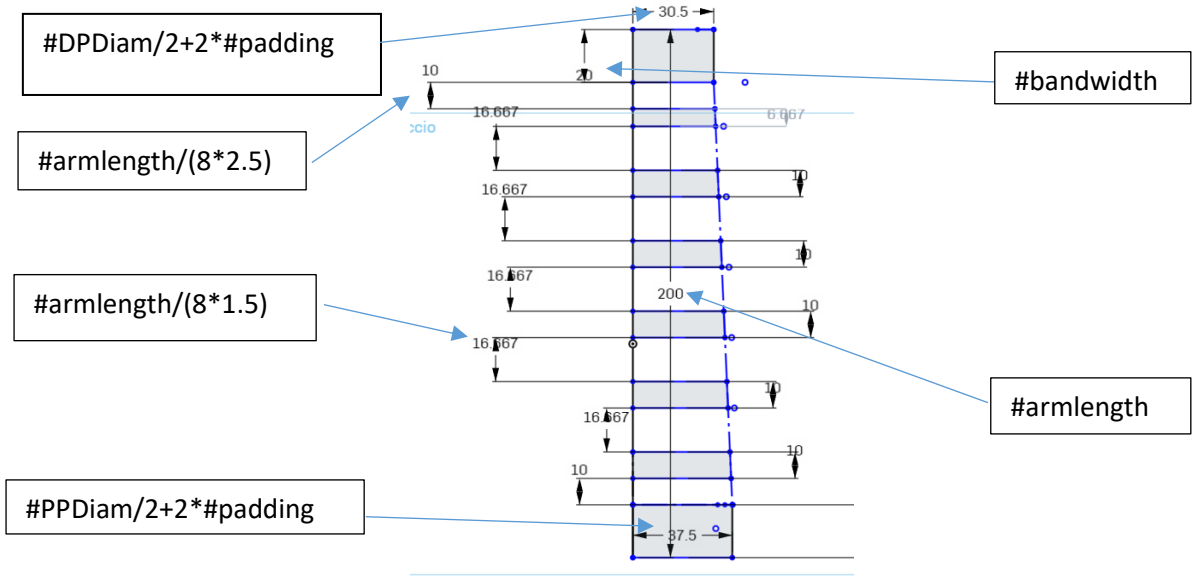

Figure 6.1 sketch 1

The Revolve extrude feature was used, which roughs a closed profile circularly around a defined axis. (Figure 6.2)

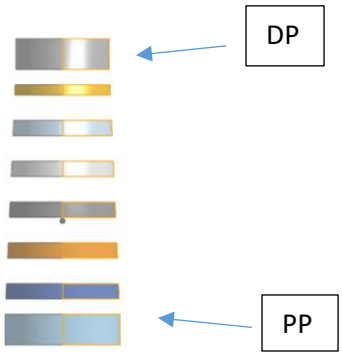

Figure 6.2

On the plane identified by the lower face of the solid DP and the upper face of the solid PP (Figure 6.2) they were drawn in sketch 2 to define the thickness of the cuff and the distance of the vertical bars (Figure 6.3).

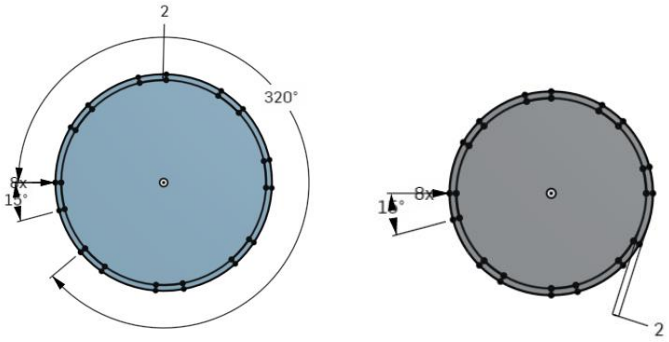

Figure 6.3 sketch 2

With the Loft function, the vertical bars were extruded (Figure 6.4) and the object was excavated by removing the parts between the internal diameters drawn in sketch 2 (Figure 6.5)

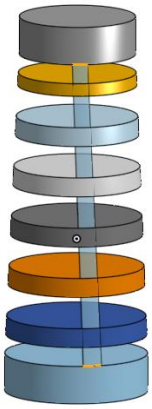

Figure 6.4

Figure 6.5

Sketch 3 fixed on the solids obtained so far, consists of the drawing of the side openings, (figure 6.6) and has been extruded to create the cracks (Figure 6.7).

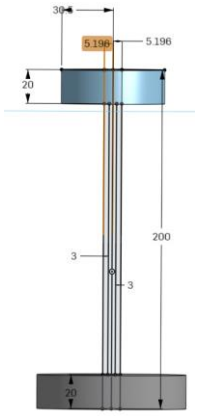

Figure 6.6

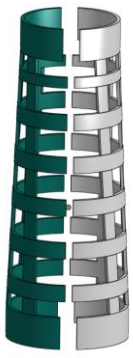

Figure 6.7

The button seat was created in a different Part Studio. A sphere with a diameter of 10 mm was drawn with the revolve command starting from the sketch of a semicircle, it was sectioned by creating a surface with an offset of 1 mm from the starting sketch, divided with the command split according to this plane and removing the resulting solid. Finally, a 5mm diameter cavity was created with the shell command, to obtain the seat of the button (Figure 6.8).

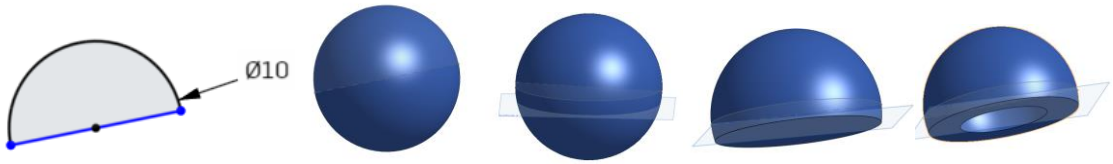

Figure 6.8

With the Import command the solid obtained in the starting model was transferred and it was positioned with the transport command through the mate connectors (Figure 6.9) .

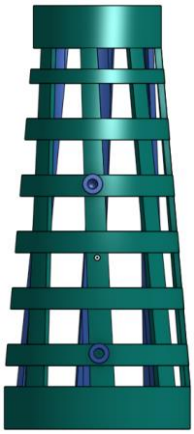

Figure 6.9

Sketches were made to create the thin connection band (Figure 6.10), with measurements always expressed in functions of variables, and to create the closure of the device Figure (6.11), with a thinning to facilitate the use of the stapler for fix the Velcro, both on the DP and PP faces and were extruded using the loft command.

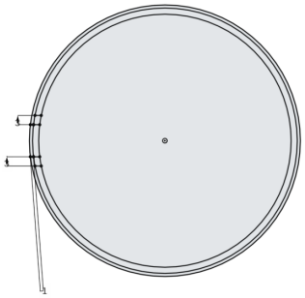

Figure 6.10

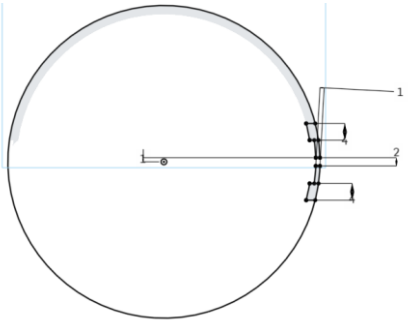

Figure 6.11

Connections were then made near the thin band and the opening, with a 2 mm fillet radius (Figures 6.12).

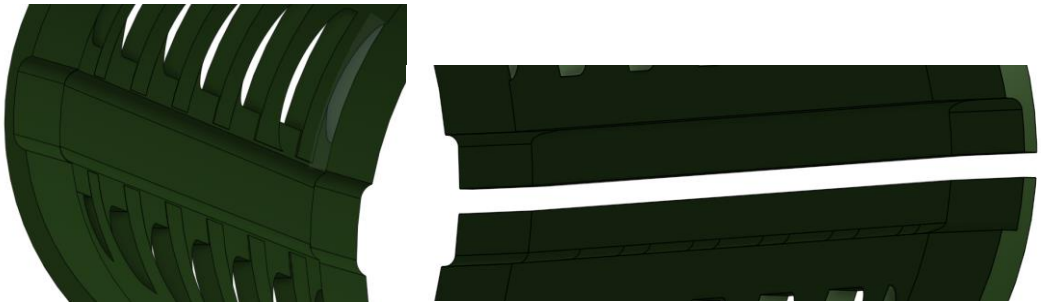

Figure 6.12

Finally, the openings along the entire structure were fillet with a 10 mm radius, to create an arched conformation and make printing easier (Figure 6.13).

Figure 6.13

APPENDIX B

A sketch was made for the electronics box (Figure 6.14) based on the measurements of the electronic board with a tolerance of 1 mm, and a thickness of the profile of 5 mm.

It was extruded with a margin height of 10 mm and a base height of 1.5 mm. Circumferences with a diameter of 3 mm were then drawn positioned at the apexes of the box and holes were created with the extrude-remove command (Figure 6.15).

Finally, a lateral opening was created (Figure 6.16) to allow the passage of the wiring with a width of 10 mm. The final result is shown in Figure 6.17..

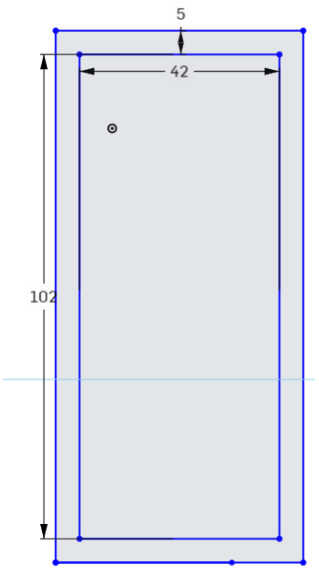

Figure 6.13

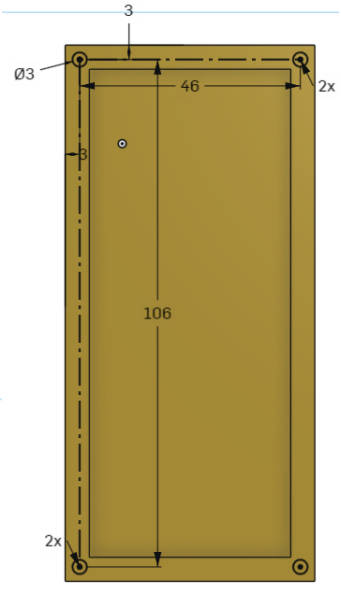

Figure 6.14

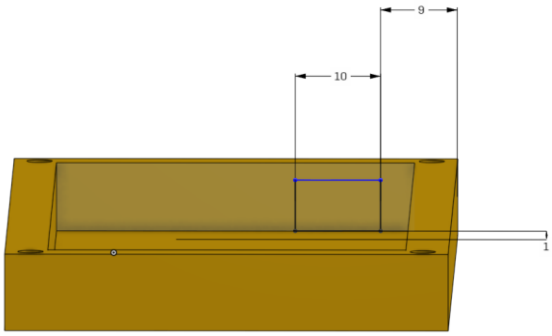

Figure 6.15

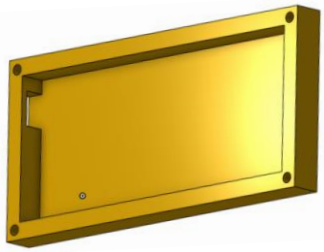

Figure 6.16

The lid was made with the external dimensions of the box and with a thickness of 2 mm. Holes were made in correspondence with the holes in the box (Figure 6.18), then chamfered (Figure 6.19) to allocate the head of the screws.

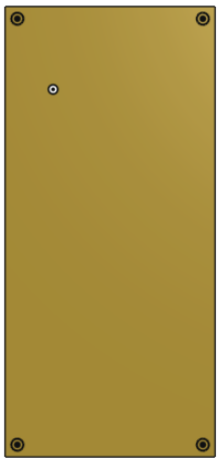

Figure 6.17

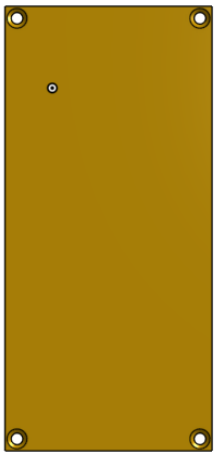

Figure 6.18

As regards the box for the removable battery, we started with the definition of the measurements of a rechargeable lithium battery (Figure 6.20)

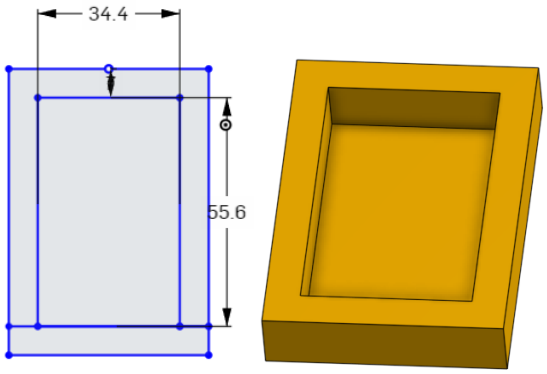

Figure 6.19

Guides have been made to allow the sliding of the lid (Figure 6.21) and the holes for the interlocking (Figure 6.22)

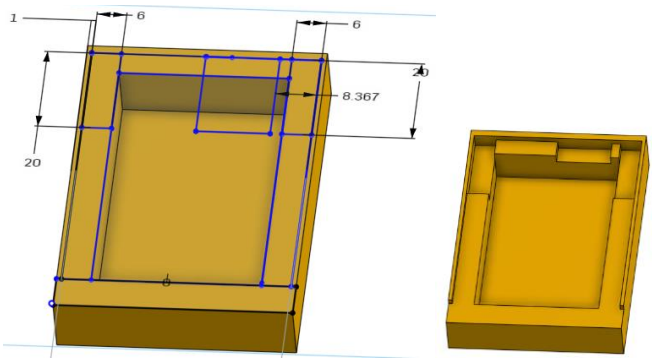

Figure 6.20

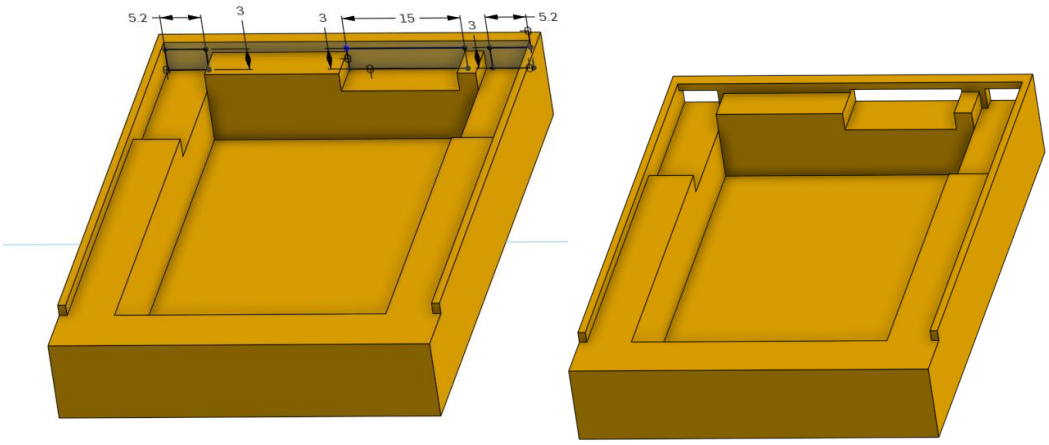

Figure 6.21

The seat for the connector was then created, sized to the model of the BlackBerry Curve 8520 Figure (6.23)

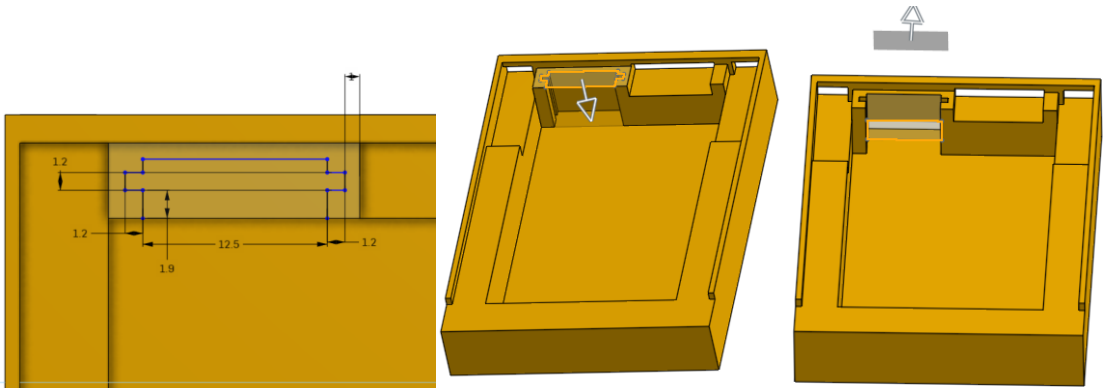

Figure 6.22

A bevel was then made on the rear side to facilitate the extraction of the battery (Figure 6.24).

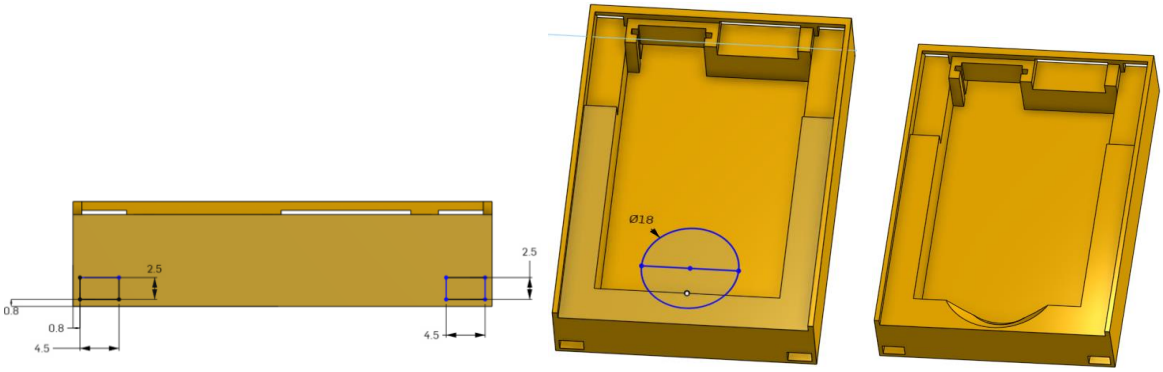

Figure 6.23

The lid was made in context with the base (Figure 6.25), to ensure correct sliding. Subsequently, protrusions were made for the interlocking with a tolerance of 0.2 mm with respect to the holes made in the base (figures 6.26).

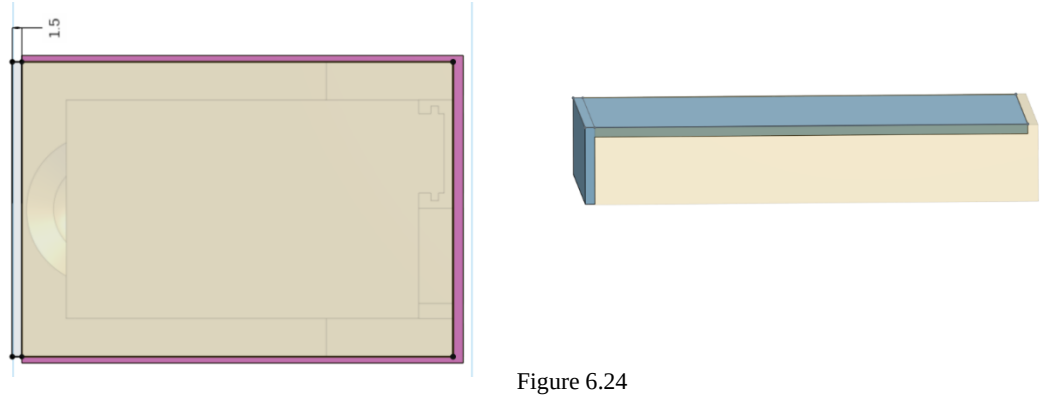

Figure 6.24

Figure 6.25

Three protrusions were created for the frontal part, on one of which a triangular profile was extruded to tighten the closure (Figure 3.27) .

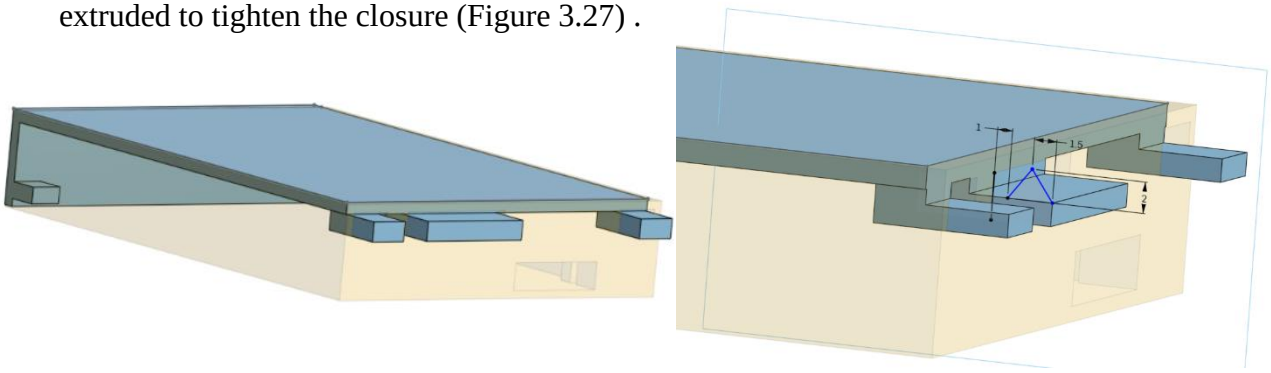

Figure 6.26

The final aspect is shown in Figure 6.28

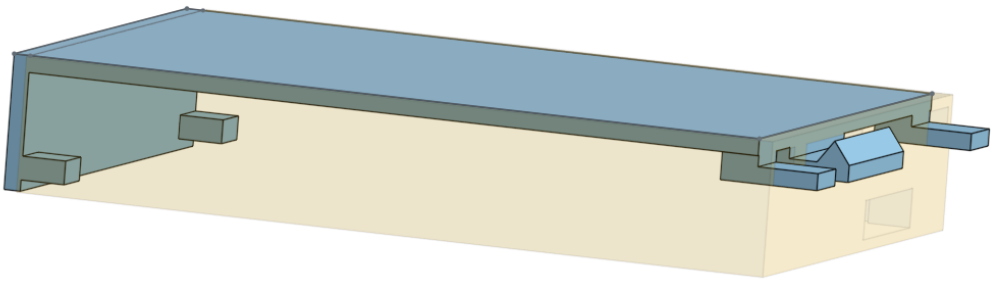

Figure 6.27